

# Define a Consistent Strategy to Model Ground Motion: Consistency in Model Parameters

Report produced in the context of the Global Project  
“GEM Ground Motion Prediction Equations”

Sinan Akkar<sup>1</sup>, John Douglas<sup>2</sup>, Carola Di Alessandro<sup>3</sup>, Ken Campbell<sup>4</sup>, Paul Somerville<sup>5</sup>, Fabrice Cotton<sup>6</sup>, Walter Silva<sup>7</sup>, Jack Baker<sup>8</sup>

<sup>1</sup> Middle East Technical University, <sup>2</sup> BRGM, <sup>3</sup> PEER, <sup>4</sup> EQECAT, <sup>5</sup> URS Corporation and Macquarie University, <sup>6</sup> Université Joseph Fourier, <sup>7</sup> Pacific Engineering and Analysis, <sup>8</sup> Stanford University





# Define a Consistent Strategy to Model Ground Motion: Consistency in Model Parameters

-

## GEM Ground Motion Prediction Equations

Version: [1.0]

Author(s): Sinan Akkar, John Douglas, Carola Di Alessandro, Kenneth W. Campbell, Paul Somerville, Fabrice Cotton, Walter Silva, Jack Baker

Date: March 2013

Copyright © 2013 Sinan Akkar, John Douglas, Carola Di Alessandro, Kenneth W. Campbell, Paul Somerville, Fabrice Cotton, Walter Silva, Jack Baker. Except where otherwise noted, this work is made available under the terms of the [Creative Commons license CC BY 3.0 Unported](http://creativecommons.org/licenses/by/3.0/)

The views and interpretations in this document are those of the individual author(s) and should not be attributed to the GEM Foundation. With them also lies the responsibility for the scientific and technical data presented. The authors do not guarantee that the information in this report is completely accurate.

Citation: Akkar, S., J. Douglas, C. Di Alessandro, K.W. Campbell, P. Somerville, F. Cotton, W. Silva, J. Baker (2013) Define a Consistent Strategy to Model Ground Motion: Consistency in Model Parameters, report published in the context of the GEM GMPE project, available from <http://www.nexus.globalquakemodel.org/gem-gmpes>



## ABSTRACT

The project entitled Global Ground Motion Prediction Equations is funded by the Global Earthquake Model (GEM) Foundation and has the objective of recommending a harmonized suite of ground motion prediction equations (GMPEs) that can be used at the global and regional scales for seismic hazard analysis and loss estimation studies. As part of this project, Task 1a experts are commissioned to make recommendations on the critical aspects of seismological predictor parameters that are used by predictive model developers to estimate ground motions for different earthquake scenarios.

The deliverable of this task will be of use for Tasks 2 and 3 that collect and test candidate GMPEs for use in the global hazard calculations. This report consists of suggestions for what can be done within the framework of the project, by recommending pragmatic solutions to common difficulties in applying GMPEs in seismic hazard assessment. In doing so, relevant references are provided. Guidelines for future ground-motion modeling studies (i.e. parameters and approaches that the ground-motion model developers should be aiming for in the future) are also suggested. The last two chapters of this report discuss the current and future considerations of ground-motion intensity parameters by GMPEs as well as simulation methods for developing reliable simulation-based GMPEs. No new research is presented in this report – recent research in this field is summarized.

Keywords: GMPE, attenuation, ground motion, hazard

## **ACKNOWLEDGEMENTS**

This study was funded by the GEM Foundation as part of the Pacific Earthquake Engineering Research Center's (PEER's) Global GMPes project. Any opinions, findings, and conclusions or recommendations expressed in this material are those of the authors and do not necessarily reflect those of the sponsors.

## TABLE OF CONTENTS

	Page
ABSTRACT .....	ii
ACKNOWLEDGEMENTS .....	iii
TABLE OF CONTENTS .....	iv
LIST OF FIGURES .....	vi
LIST OF TABLES .....	vii
<b>1 Introduction .....</b>	<b>1</b>
<b>2 Consideration of Seismotectonic Regions .....</b>	<b>3</b>
2.1 Stable Continental Regions .....	4
2.2 Subduction Zones, including Intraslab and Interface Earthquakes .....	4
2.3 Active Shallow Crustal Regions .....	5
2.4 Volcanic Zones .....	5
2.5 Deep Focus Non-Subduction Earthquakes .....	5
2.6 Earthquakes with Mainly Oceanic Travel Paths (e.g., Portugal) .....	6
<b>3 Consideration of Magnitude Type and Magnitude Range .....</b>	<b>7</b>
3.1 Magnitude Type .....	7
3.2 Magnitude Bounds .....	8
<b>4 Consideration of Source-to-Site Distance Measures .....</b>	<b>11</b>
4.1 Models Common Source-to-Site Distance Measures in GMPEs .....	11
4.2 Where Available Distance Conversations Relationships .....	12
4.3 Challenges and Approaches to Ensure Consistent Hazard Computation .....	14
<b>5 Consideration of Style of Faulting .....</b>	<b>19</b>
5.1 Challenges Styles of Faulting Classification Approaches .....	20
5.2 Influence of Database Distribution on Style of Faulting-based Ground Motion Amplitudes .....	21
5.3 The Issue of Providing Consistence in Style of Faulting for PSHA Computations .....	23
<b>6 Consideration of Near-Fault Effects .....</b>	<b>25</b>
6.1 Directivity .....	25
6.2 Directionality .....	27
<b>7 Consideration of Other Important Parameters such as Basin Effects, Depth to Top-of-Rupture, <math>Z_{1.0}</math>, <math>Z_{2.5}</math>, Nonlinear Site Effects and <math>V_{S30}</math>-<math>\kappa</math> Correlations .....</b>	<b>29</b>
<b>8 Consideration of Dispersion about the Median .....</b>	<b>31</b>
<b>9 Consideration of Ground Motion Parameters (Intensity Measures) .....</b>	<b>33</b>

9.1	Ground Motion Parameters (Intensity Measures) of Interest in this Project .....	33
9.2	Range of Reliable Spectral Ordinates and Signal Processing .....	33
9.3	Interpolation .....	35
9.4	Horizontal Component Definitions .....	36
9.5	Other Ground Motion Parameters used in GMPEs.....	36
<b>10</b>	<b>Consideration of Simulation-based GMPEs .....</b>	<b>39</b>
10.1	Point Source Stochastic Simulation Methods .....	40
10.2	Extended Source Simulation Methods .....	40
10.2.1	Stochastic Finite Source Simulation Methods .....	40
10.2.2	Hybrid Methods to Simulate Broadband Ground Motions .....	42
10.3	Hybrid Empirical Methods.....	44
10.4	Efficiency of Simulation Methods for Simulation-based GMPEs and PSHA .....	45
	<b>References .....</b>	<b>47</b>

## LIST OF FIGURES

	Page
<b>Figure 1.1</b>	Distribution of commonly used magnitude scales in the ground-motion models before and after 2000 for GMPEs estimating PGA or spectral ordinates (SA). The source of compilation is Douglas [2011]. ..... 8
<b>Figure 4.1</b>	Yearly-based distribution of GMPEs that estimate PGA or elastic spectral ordinates (SA) for different source-to-site distance measures. .... 13
<b>Figure 4.2</b>	Magnitude-dependent distance conversion relations of Scherbaum <i>et al</i> [2004] to estimate $R_{epi}$ , $R_{hyp}$ and $R_{rup}$ from a given $R_{JB}$ . .... 14
<b>Figure 4.3:</b>	$R_{epi}$ vs. $R_{JB}$ scatters in strike-slip style-of-faulting events for different magnitude intervals and their comparisons with the average trends computed from the Scherbaum <i>et al</i> [2004] relationships. The data are gathered from the recently compiled SHARE ground-motion databank [Yenier <i>et al</i> , 2010]..... 16
<b>Figure 4.4</b>	Same as Figure 4.3 but for $R_{hyp}$ vs. $R_{JB}$ . .... 17
<b>Figure 4.5</b>	Same as Figure 4.4 but for $R_{rup}$ vs. $R_{JB}$ ..... 18
<b>Figure 5.1</b>	Given a set of GMPEs, the normal and reverse spectral ordinates for a rock site ( $V_{S30} = 760$ m/sec) that are normalized by the corresponding strike-slip spectral ordinates (i.e., N:SS and R:SS, respectively). The magnitude of scenario earthquake is $M_w$ 7. The fault rupture is assumed to emerge at the surface. The abbreviations AS08, BA08, CB08, CY08 and AB10 that are given in the graph legend refer to Abrahamson and Silva [2008], Boore and Atkinson [2008], Campbell and Bozorgnia [2008], Chiou and Youngs [2008] and Akkar and Bommer [2010], respectively. .... 20
<b>Figure 5.2</b>	Magnitude ( $M_w$ ) vs. distance ( $R_{JB}$ ) scatter of the datasets used for the case studies. .... 22
<b>Figure 5.3</b>	Normal to strike-slip (N:SS) and reverse to strike-slip spectral ordinate ratios for the three cases that are studied for investigating the sensitivity of database distribution in the estimated ground-motion amplitudes for different SoF. The sudden drop in R:SS after $T = 2$ sec can be due to sparse data and should be considered with caution..... 23



## LIST OF TABLES

### Page

<b>Table 5.1</b> Classification schemes for style-of-faulting (modified from Bommer <i>et al</i> [2003]).....	24
---	----



## 1 Introduction

Ground-motion prediction equations (GMPEs) relate a ground-motion intensity measure to a set of explanatory variables describing the source, wave propagation path and site response. Although these estimator parameters mainly include the magnitude, style-of-faulting and source-to-site distance, there are significant efforts to include additional variables to model the ground-motion behavior in a more realistic way. These variables have different levels of influence on the estimated ground-motion intensity measure. Moreover, each of these variables is affected by different factors that in turn define the level of accuracy of the predictions. This report addresses the important aspects these estimator parameters in different chapters that can be of use for the selection of GMPEs among a set of candidate models for reliable regional and global seismic hazard assessment. To this end, members of Task 1a suggest a set of recommendations for the optimum performance of each major predictor parameter and highlight the required features of these parameters as well as the predictive models that are believed to lead a consistent seismic hazard assessment. The report also includes the considerations of Task 1.a members on ground-motion intensity parameters and generation of synthetic accelerograms for developing simulation-based GMPEs. The companion report of Douglas *et al* [2011] presents a pre-selection of candidate GMPEs for the same project based on the recommendations made in Task 1a.



## 2 Consideration of Seismotectonic Regions

Acceptable ground-motion models must consider the differences between the main tectonic regimes that are listed in the following paragraphs. The models should address the important features of fault mechanisms and source properties that characterize each tectonic regime. Furthermore, models should consider differences in the attenuation of ground-motion amplitudes and in important estimator parameters that can be of particular use for a seismotectonic region. During a hazard study, it is very important to consider the seismotectonic setting for which a model was developed. There are several cases in which a certain event is associated with different seismotectonic regions by different authors. For example, the 2008 Wenchuan Earthquake is defined as being associated with either a Stable Continental Region (SCR) or a Shallow Active Crustal region in the special issue of the Bulletin of the Seismological Society of America (Vol. 100, No.5B), which may reflect the occurrence of the earthquake at a boundary between such regions.

In a report for the GEM1 project Douglas *et al* [2009] proposed a rough seismotectonic zonation for the entire globe based on the Flinn-Engdahl (FE) regionalization. The zonation of Douglas *et al* [2009] was provided to GEM1 in the form of a Matlab viewer and associated data files. The FE regionalization was used for consistency with standard seismological practice and because of the easy availability of the associated polygons. FE regionalization divides the Earth into over 700 zones based on political and tectonic provinces and hence it was considered by Douglas *et al* [2009] as an appropriate choice (if slightly too detailed some areas) for GEM1. Douglas *et al* [2009] assessed whether the five types of seismicity for which they proposed GMPEs (active, subduction, SCR, volcanic and Vrancea-type) could occur in each FE region based on the work of Johnson *et al* [1994], Bird [2003] and their own knowledge. If they considered that a type of seismicity was possible in a given FE region then non-zero weights were assigned to the GMPEs they had proposed for such a tectonic regime. This procedure was followed for all five tectonic types and all 700+ FE zones. This approach means that each zone can be associated with more than one type of seismicity, which is necessary because of the Earth's complex tectonics. FE regions for oceanic areas far from land were assigned to a sixth category (Ocean) and no GMPEs were assigned.

As part of WP3 of SHARE (Seismic Hazard Harmonization in Europe) project [1] and following much internal and external discussion, a seismotectonic zonation map was developed for use in selecting the appropriate GMPEs for all locations in Europe, the Mediterranean and the Middle East [Basili *et al*, 2011]. Basili *et al* [2011] used various global and regional databases on geology, tectonics, seismicity, crustal structure and kinematics to classify locations into: active and stable zones. They then split active zones into dipping slab and deep source, compression and accretion wedge, extension, mixed, strike-slip and transform, spreading ridge, magmatic province and volcanoes; and they further divided the stable zones into shield, continental and oceanic. Unlike the GEM1 regionalization, Basili *et al* [2011] did not base their zones on the FE regionalization but chose the polygons themselves – this makes their approach much more flexible. Their regionalization is available in Geographical Information Systems (GIS) format.

In the framework of the GEM Global GMPEs-PEER project, we chose to identify the below major seismotectonic regions. We believe that, for consistent regional and global hazard assessment, the chosen

candidate GMPEs for each region should fairly account for the relevant discussions that are given in the following subsections.

## 2.1 Stable Continental Regions

There are a number of different classifications that describe stable continental regions (SCRs). The most widely used classification, based on contrasts in age, tectonic origin and tectonic history, is the one developed by EPRI (Johnston *et al* [1994]). This classification was motivated by the desire to find regions of the earth that might be analogous to the central and eastern United States and thus provide additional data and insight into the nature of earthquakes in stable continental regions. The EPRI classification was not based on observations of contrasting earthquake source or seismic wave propagation characteristics, although it implied that such contrasts might result from contrasts in tectonic origin and history. The developers of GMPEs in stable continental regions are now in the process of discovering the degree to which this conjecture is borne out in the actual earthquake source and seismic wave propagation characteristics of these regions. As part of a global effort, our classification needs to be consistent with the other GEM Global and Regional Hazard Components (e.g., in strain rates). For example, in the SHARE [1] project, one of the regional components of GEM, the tectonic regions in Europe are globally separated into shield (cratonic - low deformation with low attenuation) and continental crust (non cratonic - low deformation but significant attenuation). A similar distinction between tectonic regions was independently identified by Somerville *et al* [2009] in the course of developing GMPE's for Australia. They developed separate GMPEs for the cratonic regions (with low deformation and low attenuation) and non-cratonic regions (with low deformation and high attenuation) of Australia. An attempt towards using separate GMPEs for cratonic and non-cratonic regions is also presented by Delavaud *et al* [2012].

There is evidence that earthquakes in stable tectonic regions have source characteristics that differ in systematic ways from those of earthquakes in tectonically active regions. For example, the rupture areas of earthquakes in stable continental regions [Somerville *et al*, 2001] are about half those of crustal earthquakes in tectonically active regions [Somerville *et al*, 1997], implying larger slip and larger static stress drop. The slip durations of stable continental region earthquakes are correspondingly longer, but not long enough to make their slip velocities as low as those of earthquakes in tectonically active regions. This evidently gives rise to slightly higher ground motion levels for earthquakes in stable continental regions than in tectonically active regions. Such differences in rupture area are also reflected in the earthquake source scaling relations developed by Leonard [2010]. The results of Radiguet *et al* [2009] also show that the degree of structural maturity of the long-term faults is a factor that probably plays a significant role in the amplitudes of strong ground motion (i.e., when rupturing in large earthquakes, immature faults produce larger ground-motions than mature faults that break in a similar magnitude events).

## 2.2 Subduction Zones, including Intraslab and Interface Earthquakes

There is also a need for setting a consistent definition for differentiating between different types of earthquakes associated with a subduction zone (e.g., using depth and focal mechanism).

Acceptable ground-motion models should take into consideration the differences existing among, for instance, interface and intraslab earthquakes, and provide separate sets of coefficients for each type of earthquake. This implies that the metadata database should maintain accuracy in providing reliable information on earthquake depth and focal mechanism.

Some recent models [McVerry *et al*, 2006; Zhao, 2010; Dhakal *et al*, 2010; Abrahamson *et al*, 2012] have started to include modifications for the high attenuation related to the back arc region of the subduction zone (cases of Cascadia, New Zealand and Japan).

### 2.3 Active Shallow Crustal Regions

This type of region is characterized by active tectonics with relatively high strain rates, generally close to plate boundaries, and earthquakes that occur in the upper 20 to 30 km of the crust generally on well-identified mature faults (e.g., California, Italy, Turkey, Greece and Japan). It is often considered that ground motions associated with this type of seismotectonic regime do not show strong regional dependencies, at least for moderate and large earthquakes (e.g., Italian ground motions are on general similar to those in California for the same magnitude, distance, site class and mechanism). The vast majority of published GMPEs were derived for this type of area (partly because of the considerable amount of strong-motion data that are available). Hence one of the main difficulties in hazard studies is to reduce the number of available GMPEs down to a more manageable number while retaining sufficient models to account for the epistemic uncertainty. This topic will be discussed to some extent in Task 2 report [Douglas *et al*, 2012].

### 2.4 Volcanic Zones

Volcanic earthquakes are unlikely to be larger than about  $M_w$  5.5 (and probably much smaller) and, therefore, the seismic hazard from this type of earthquake is unlikely to be important on a global scale. In fact there are almost no ground-motion models specifically estimating the ground-motion amplitudes for volcanic eruptions. Although the GMPEs by McVerry *et al* [2006] and Zhao [2010], which is the modification of Zhao *et al* [2006] use acceleration recordings of volcanic events, they are mainly derived for crustal and subduction earthquakes. De Natale *et al* [1998] proposed a stochastic model for estimating the ground motions of volcanic events in Italy.

As one of the regional components of GEM, the SHARE [1] project decided to adopt the approach implemented in the current Italian national seismic hazard maps while addressing the hazard in Volcanic regions [see Montaldo *et al*, 2005]. This approach consists of introducing separate GMPEs within a seismic source zone of limited extension surrounding a volcano with well-documented historical evidence of damaging earthquakes, such as the Mount Etna volcano, in Sicily. Such GMPEs should be able to deal with events of shallow focal depth, from 2 to 5 km. A specific analysis was carried out on the acceleration recordings of moderate earthquakes ( $3.2 < M_w < 4.5$ ) from recent Italian events, particularly in the Mount Amiata (southern Tuscany) and Mount Etna areas. The results of this study showed that the use of recent ground-motion model of Faccioli *et al* [2010] is appropriate for such regions.

### 2.5 Deep Focus Non-Subduction Earthquakes

Deep focus (non-subduction) earthquakes are seen in Vrancea (Romania) zone [Wortel and Spakman, 2000] as well as the New Hebrides Islands [Chatelain *et al*, 1992], Baja California [Burkett and Billen, 2009], Bucaramanga (Colombia) [Frohlich *et al*, 1995], eastern Anatolia [Facenna *et al*, 2005], New Guinea [Cloos *et al*, 2005] and Pamir Hindu-Kush [Levin *et al*, 2002]. In such seismotectonic regions slab delaminating and detachment phenomena are present that cause the occurrence of deep earthquakes. Currently there are no specific ground-motion models that can successfully pass the rigorous pre-selection criteria highlighted by

Task 2 for such seismotectonic regions. In fact, the only model that exists for such a region is the one developed by Sokolov *et al* [2008], but its implementation on a global scale PSHA study is made extremely difficult due to the strong azimuthal dependence of the site coefficients, which are specific to the Vrancea region. The hazard analysts can use GMPEs of intraslab earthquakes for these regions.

## **2.6 Earthquakes with Mainly Oceanic Travel Paths (e.g., Portugal)**

For offshore seismic hazard studies, a mixture of GMPEs from active and SCRs may be recommended as such regions also lack GMPEs that specifically feature the earthquake source and wave-propagation characteristics of these regions. Studies by Atkinson [2010], Munson and Thurber [1997] and Wong [1990] can also be of relevance for estimating hazard in such regions.



### 3 Consideration of Magnitude Type and Magnitude Range

#### 3.1 Magnitude Type

Moment magnitude ( $M_w$ ) has almost become the standard magnitude scale in the current practice for developing GMPEs. It can describe the energy release of an earthquake without suffering from saturation, which is not the case for other magnitude scales<sup>1</sup>. This observation can be appreciated from the histogram plot given in Figure 1.1 that shows the distribution of GMPEs that employ commonly known magnitude scales before and after 2000. The data are gathered from the collection of GMPEs published by Douglas [2011]. The statistics in this figure display the number of pre- and post-2000 GMPEs estimating PGA or spectral ordinates (abbreviated as SA). Although the use of  $M_w$  shows a significant increase during the last decade, GMPEs that use  $M_L$  (local magnitude) as well as  $M_s$  (surface-wave magnitude) still constitute a fairly large fraction in the overall number of GMPEs. Models that use  $M_L$  are generally local GMPEs whereas many earlier global predictive equations as well as few local ones have used  $M_s$  as the magnitude definition since it is one of the most frequently used magnitude measures reported in earthquake catalogs. Therefore conversions between magnitude scales are necessary when the magnitude definitions of the GMPEs differ. Such situations are still common in practice, in particular, for regions where no region-specific and reliable predictive models exist. Although there are quite a few peer-reviewed empirical relations that convert various magnitude scales to a common magnitude definition (e.g., moment magnitude) [Utsu, 2002], they can differ significantly in estimating the target magnitude scale (Figure 1.1 and Figures 17 to 22 in Utsu, [2002]). These relations carry their own uncertainty due to different regression methods adopted in their calculation as well as the different approaches used in the computation of magnitude scales by different seismic agencies. This situation is particularly important when dealing with the predictive models that use  $M_L$  as the independent magnitude parameter because this magnitude scale can vary significantly from one region to the other. The original definition of  $M_L$  proposed by Richter [1935] has been adopted in different ways by various seismic agencies around the world depending on the technical capacities of the seismic instruments [Utsu, 2002]. Thus, conversions between any magnitude scale and  $M_L$  should to be done using the empirical relationships derived from the region of concern.

State-of-the-art seismic-hazard analyses do consider error propagation due to the aleatory and epistemic uncertainties inherent in magnitude scaling relationships when GMPEs that use different magnitude definitions have to be converted to a common magnitude format. Bommer *et al* [2005] made a detailed

---

<sup>1</sup> The local magnitude ( $M_L$ ) can be a better representative of stress drop taking into account the near field/distance effect. However, to make consistency among different models and to make the best use of information in terms of source characterization, geological slip rate of the faults and its relation to earthquake magnitude  $M_w$  is still the most efficient magnitude scaling.

discussion on this issue for both deterministic and probabilistic seismic hazard analysis. The authors also presented the variations in the standard deviations of some of the GMPEs selected in their study (Figure 3 in the referred article) indicating that error propagation due to magnitude conversion has a larger influence at longer spectral periods because of the stronger magnitude dependence of ground motions at these periods.

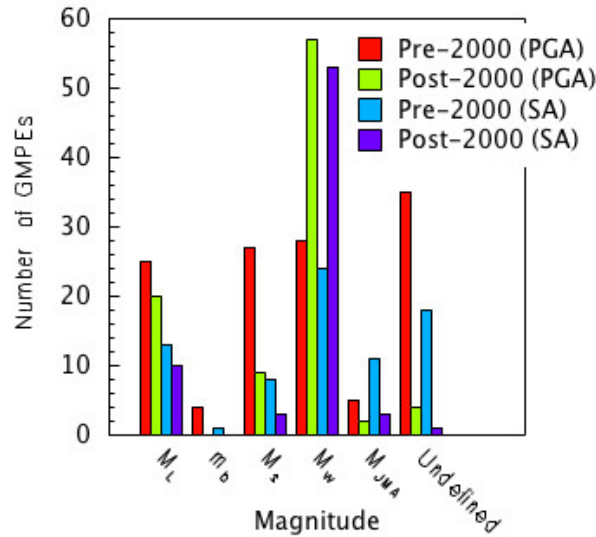


**Figure 1.1** Distribution of commonly used magnitude scales in the ground-motion models before and after 2000 for GMPEs estimating PGA or spectral ordinates (SA). The source of compilation is Douglas [2011].

The most straightforward way to avoid such complications in hazard analysis is to employ GMPEs that use  $M_w$  as the magnitude parameter. On the other hand, if ideal conditions cannot be developed for reasons summarized in the above paragraph and if there is a need to use GMPEs of different magnitude definitions the analyst should then convert different magnitude definitions to  $M_w$ . In such situations, one way of understanding the modeling uncertainty stemming from magnitude conversions is to observe the differences in spectral ordinate estimates after the application of alternative magnitude conversion relations. Global earthquake catalogs that report the size of recorded events in a reliable manner would reduce the modeling uncertainty in magnitude conversion relations and provide a valuable opportunity to develop GMPEs having consistent magnitude scaling. The development of earthquake catalogs having homogenous and reliable magnitude scaling is being done by the GEM Instrumental Catalogue Hazard component.

### 3.2 Magnitude Bounds

Another important concern in ground-motion models is the consideration of upper and lower magnitude bounds. In seismic prone regions causal relationships between earthquakes and potential seismogenic features of the region define the seismic activity that in turn describes region-specific magnitude bounds. Thus, ground-motion models should be devised to address these magnitude ranges. This is particularly important for seismic hazard analysis since it provides the future ground-motion demands to the engineering community by using GMPEs. Consequently, the description of magnitude bounds in hazard analysis should also consider the constraints imposed by engineering practice as the engineering community justifies the rationale behind the ground-motion demand by assessing the vulnerability of structural systems against

earthquake activity; notwithstanding the limitations in strong-motion databases that are used for deriving predictive models also play an important role in defining the magnitude bounds in GMPEs.

Except for local models that generally estimate ground motions occurring in a restricted region, thus focusing mainly on small local events within a narrow magnitude range, most of the GMPEs are based on the moderate-to-large magnitude earthquakes having lower magnitude threshold limits approximately equal to or greater than 5. There might be several reasons behind such a preference. Firstly, current ground-motion models generally rely on triggered recordings obtained from analog or early digital accelerographs that can record earthquakes of magnitudes 5 and above. Such data still constitute an important fraction of strong-motion databases. Another important factor behind this choice can be the general consensus among the engineering and seismological communities that most structures are susceptible to damage for magnitude levels greater than 5, which leads the model developers to select events starting from magnitude 5. Finally, the increased uncertainty in the magnitude determination of small events as well as the difficulty in acquiring their source characteristics also play a role in the choice of relatively larger magnitudes as the lower magnitude limit in most GMPEs. However, it has already been recognized that ground-motion models derived from moderate-to-large magnitude earthquakes tend to overestimate the ground motions from small magnitude events, which is of particular importance when computing the hazard for regions of low-to-moderate seismicity [Atkinson and Morrison, 2009; Chiou *et al*, 2010; Campbell, 2011; Cotton *et al*, 2008]. Moreover recent studies have shown that empirical GMPEs often overpredict spectral ordinates not only at smaller magnitudes but also at the lower magnitude limit of their original datasets [Bommer *et al*, 2007; Cotton *et al*, 2008; Atkinson and Morrison, 2009; Chiou *et al*, 2010]. These findings suggest that the use of GMPEs below their lower magnitude bound may result in erroneous hazard computations. Therefore, extending the current GMPEs towards lower magnitudes or deriving new GMPEs by considering relatively lower magnitude levels, contingent on the reliability of metadata information, would reduce the adverse effects as discussed above. Various model developers have already updated their recent GMPEs to account for the ground-motion amplitudes of smaller events [e.g., Chiou *et al*, 2010; Atkinson and Boore, 2011] and the current PEER NGA-West2 [4] project is addressing this issue for all of the NGA prediction equations. Given the current improvements in strong-motion databases, the new predictive models can choose the lower magnitude level as  $M_w$  4 or  $M_w$  4.5 for subduction and active crustal regions that host most of the seismic activity around the globe. Douglas and Jousset [2011] presented a novel idea (based on stochastic models) to extend the current GMPEs towards lower magnitude levels for their effective use in seismic hazard assessment or for testing the GMPEs against empirical data collected from regions of low-to-moderate seismicity. This novel idea could be developed into a consistent strategy for the efficient use of GMPEs for stable continental, volcanic and deep-focus non-subduction regions of moderate-to-low seismicity where small-magnitude data are abundant.

The upper bound magnitude values generally range between 7 and 8 for most of the recently developed global ground-motion models. This magnitude range reflects the likely maximum magnitudes that can be expected in most of the seismically-active sources all around the world. Nevertheless, as indicated in the previous paragraph, the magnitude ranges depend on the seismicity of tectonic regions and the recent devastating earthquakes ( $M_w$  8.8 Maule, Chile, and  $M_w$  9.0 Tohoku-oki, Japan, earthquakes) showed that the maximum magnitude values can be well above  $M_w$  8 for subduction earthquakes. These new observations as well as more refined geological and paleoseismic studies will eventually push the upper bound magnitude level above 8 in the future GMPEs pending the accumulation of such data in the strong-motion databases. Nevertheless, in view of the state of practice in the use of current GMPEs, the maximum magnitudes to be considered in stable continental and shallow crustal active regions should be in the range of  $M_w$  8. This upper

bound should be at least  $M_w$  8.5 for most subduction interface earthquakes. The ground-motion models that are going to be tested over these major tectonic regimes should be suitable for these maximum magnitude levels and they should not be extrapolated more than half  $M_w$  unit beyond their applicability range because otherwise misleading ground-motion levels could be predicted. For large magnitude (i.e.,  $M_w$  +9) subduction events one approach could be the generation of synthetics for the evaluation of hazard as the upper bound magnitude limits of current GMPEs cannot cover such large magnitude ranges. However, the applicability of this method is not warranted within the context of GEM-PEER global GMPEs project.

## 4 Consideration of Source-to-Site Distance Measures

### 4.1 Models Common Source-to-Site Distance Measures in GMPEs

The common source-to-site distance measures in the ground-motion predictive models are  $R_{\text{epi}}^2$ ,  $R_{\text{hyp}}^1$ ,  $R_{\text{rup}}^1$  and  $R_{\text{JB}}^1$  although the latter two distance metrics have become popular in recent GMPEs as they can address the variation of ground-motion amplitude more appropriately for large events at sites closer to the source. Both  $R_{\text{rup}}$  and  $R_{\text{JB}}$  are extended-source distance measures and their calculation requires reliable finite-fault (or rupture model) representations that are generally available for large-magnitude earthquakes or for some specific events that are studied individually [e.g., Cauzzi *et al* 2011]. Currently seismic agencies routinely report the hypocenter (epicenter and focal depth) for the majority of earthquakes of engineering concern. Consequently the point-source distance measures (i.e.,  $R_{\text{epi}}$  and  $R_{\text{hyp}}$ ) are still more accessible in the existing strong-motion databases, resulting in a larger number of GMPEs that use either  $R_{\text{epi}}$  or  $R_{\text{rup}}$  as distance measures. This fact is illustrated in Figure 4.1 that shows the worldwide ground-motion models developed up to 2010 for different distance metrics. The presented statistics are extracted from Douglas [2011] and they show the number of ground-motion models estimating PGA or spectral ordinates (abbreviated as SA) for the time intervals before and after 2000. As it can be appreciated from this figure most of the pre-2000 models are based on  $R_{\text{epi}}$  and  $R_{\text{hyp}}$ . The number of GMPEs that use extended-source distance measures increases significantly after 2000 due to the refinements in the ground-motion databases both at the country [e.g., Luzi *et al*, 2008; Akkar *et al*, 2010] and global [Ambraseys *et al*, 2004; Power *et al*, 2008] levels. Nevertheless the number of models that have been developed using  $R_{\text{epi}}$  and  $R_{\text{hyp}}$  are still considerable in the post-2000 period. These are generally local GMPEs whereas ground-motion models that employ extended-source distance measures are primarily derived from global strong-motion databases. This is because such databases are generally developed under the framework of well-funded projects that can recruit experts on database compilation and processing. The histogram in Figure 4.1 also reveals the existence of a large number of hybrid GMPEs that combine either  $R_{\text{JB}}$  and  $R_{\text{epi}}$  or  $R_{\text{rup}}$  and  $R_{\text{hyp}}$  pairs because both  $R_{\text{epi}}$  and  $R_{\text{hyp}}$  can be the proxies of  $R_{\text{JB}}$  and  $R_{\text{rup}}$ , respectively for small magnitude events whose fault-plane solutions are rarely available in the earthquake catalogs; one of the most significant limitations in the current earthquake catalogs.

---

<sup>2</sup>  $R_{\text{epi}}$ : epicentral distance;  $R_{\text{hyp}}$ : hypocentral distance;  $R_{\text{rup}}$ : closest distance to the rupture;  $R_{\text{JB}}$ : closest horizontal distance to the vertical projection of the rupture.

## 4.2 Where Available Distance Conversations Relationships

Whenever ground-motion models of different distance metrics are employed in probabilistic seismic hazard analysis (PSHA), the state-of-art practice is to adjust the differences in distance measures to model consistent earthquake scenarios. Moreover GMPEs that use extended source distance metrics should be modified properly while addressing the hazard in the background seismicity for which earthquake scenarios are treated as point sources. For such distance conversions, relationships proposed in Scherbaum *et al* [2004], EPRI [2004] or Petersen *et al* [2008] can be used. Scherbaum *et al* [2004] present distance conversion relations for shallow active tectonic regimes and for the two fundamental fault mechanisms (dipping and strike-slip faults) in terms of magnitude and distance. The proposed expressions consider  $R_{JB}$  as the reference distance metric and estimate the corresponding  $R_{epi}$ ,  $R_{hyp}$  and  $R_{rup}$  using models based on a Gamma distribution. The suggested distance conversion relations of Scherbaum *et al* [2004] are valid for  $R_{JB}$  less than 100 km and for moment magnitudes ( $M_w$ ) between 5 and 7.5. The functional forms in EPRI [2004] estimate  $R_{JB}$  or  $R_{rup}$  from a given epicentral distance. The EPRI expressions are also functions of magnitude and they are specifically derived for the ground-motion models that are used in the PSHA studies of nuclear power plants in the central and eastern United States [EPRI, 2004]. These relationships are applicable for epicentral distances less than 1000 km and for  $5 \leq M_w \leq 8$ . The EPRI expressions consider epicenter locations either as “random” (i.e., the epicenter of an earthquake is uniformly distributed on the rupture plane) or “centered” (i.e., the epicenter is centered on the earthquake rupture plane). They are derived for an equal mixture of reverse and strike-slip earthquakes. The Petersen *et al* [2008] study that updates the US National Seismic Hazard Maps describe the calculation of  $R_{JB}$  and  $R_{rup}$  for PSHA calculations by modeling the fault sources as nonplanar faults [Zeng and Chen, 2001]. This study also derives expressions for computing  $R_{JB}$  and  $R_{rup}$  from  $R_{epi}$  by assuming finite vertical or dipping faults whose strike directions are uniformly distributed from  $0^\circ$  to  $180^\circ$ ; a methodology suitable for computing the hazard in background sources. Petersen *et al* [2008] provide distance relations that are specific to the earthquake scenarios developed in PSHA studies and their approach is quite different from that of Scherbaum *et al* [2004] and EPRI [2004].

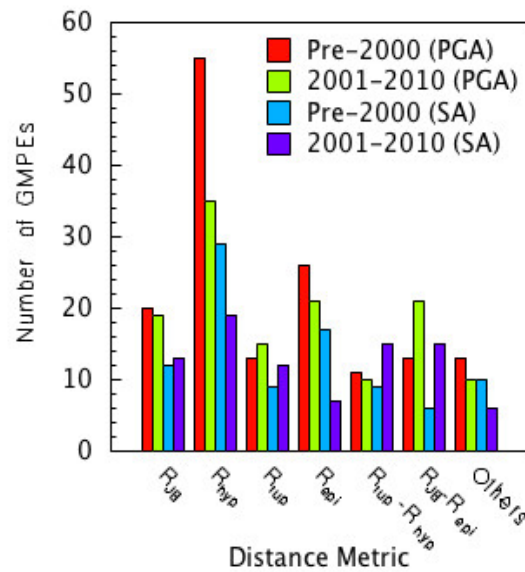


**Figure 4.1** Yearly-based distribution of GMPEs that estimate PGA or elastic spectral ordinates (SA) for different source-to-site distance measures.

Figure 4.2 presents the distance relationships proposed by Scherbaum *et al* [2004] for strike-slip style-of-faulting. The average trend lines shown in each panel indicate that the differences between the distance metrics become prominent for moderate-to-large magnitude events at locations closer to the source. Differences between  $R_{hyp}$  vs.  $R_{JB}$  and  $R_{epi}$  vs.  $R_{JB}$  are much more prominent than those of  $R_{rup}$  vs.  $R_{JB}$ . As a matter of fact for distances approximately larger than 20 km  $R_{rup}$  and  $R_{JB}$  almost overlap each other regardless of the variation in magnitude. This observation indicates that PSHA studies that rely on a mixture of extended-source and point-source distance measures may lead to misleading hazard results unless conversions between these different distance measures are made. As expected such misleading results seem to be more pronounced for low-to-moderate seismicity regions (i.e., for sites dominated by smaller magnitude events) [Bommer and Akkar, 2012].

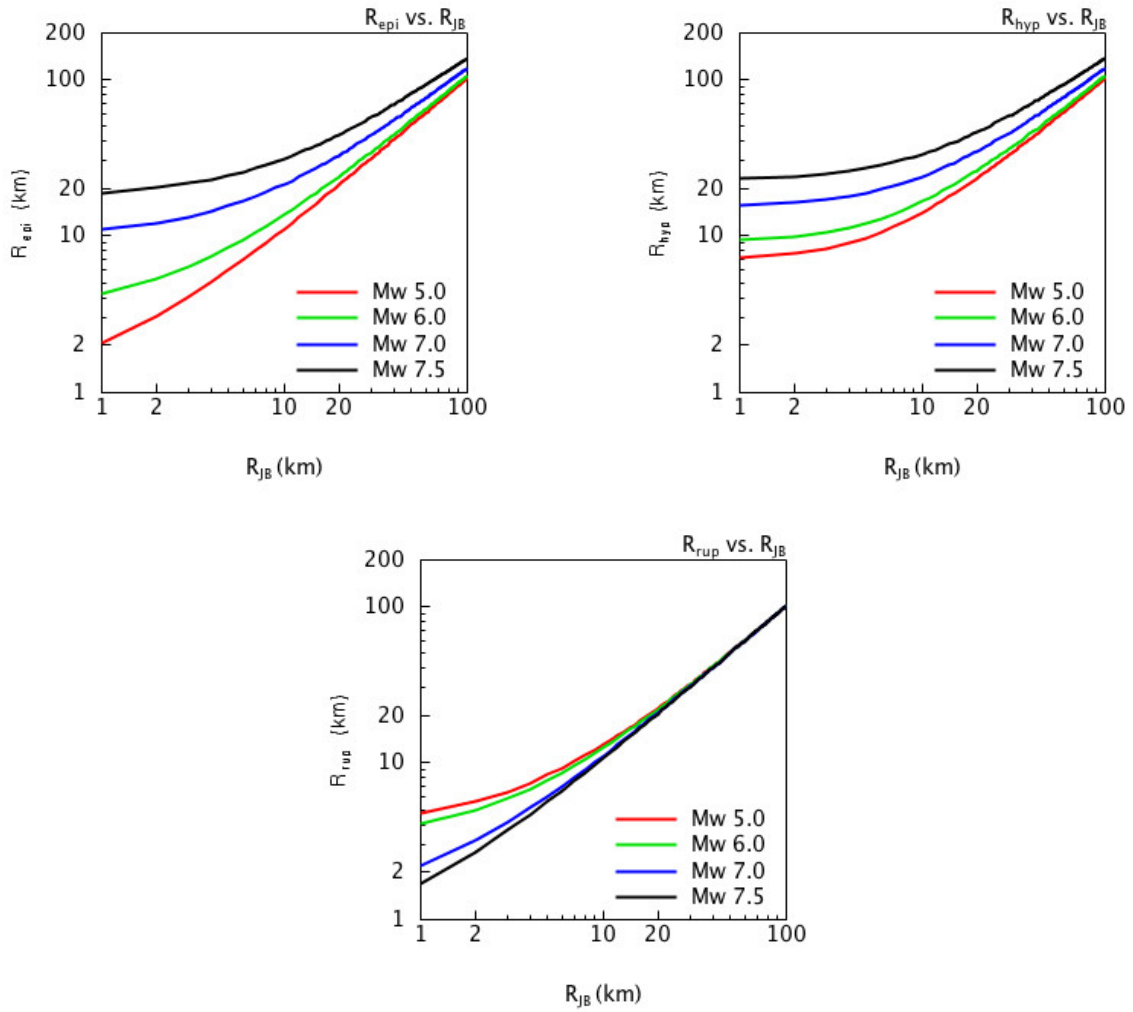


**Figure 4.2** Magnitude-dependent distance conversion relations of Scherbaum *et al* [2004] to estimate  $R_{\text{epi}}$ ,  $R_{\text{hyp}}$  and  $R_{\text{rup}}$  from a given  $R_{\text{JB}}$ .

### 4.3 Challenges and Approaches to Ensure Consistent Hazard Computation

The major challenge in employing distance conversion relations is the error propagation in the distance calculations onto the estimated ground motions. This uncertainty can lead to larger standard deviations (i.e., increased aleatory variability) in the GMPEs and may have a negative effect on the hazard [Scherbaum *et al*, 2005]. One approach to avoiding such large uncertainties in hazard calculations is to use hazard codes that are capable of modeling finite fault sources in such a way that the commonly used distance metrics can be computed and each GMPE is used with its original distance definition [Bommer *et al*, 2010]. In a similar fashion, for hazard analysis concerning areal sources (for which the earthquake scenarios are defined as points) GMPEs that use  $R_{\text{JB}}$  or  $R_{\text{rup}}$  can be employed consistently together with GMPEs that use point-source distance measures if the hazard software is capable of simulating pseudo ruptures for each earthquake scenario with random orientations and with dimensions determined from empirical relationships [Bommer *et al*, 2010; Petersen *et al*, 2008]. These alternatives depend on the computational ability of hazard software and the analyst should disregard using, for example, GMPEs of point-source distance measures for estimating ground-motion amplitudes of large faults unless the hazard software can model such sources for proper



calculation of  $R_{\text{epi}}$  or  $R_{\text{hyp}}$ . Another reasonably simple method, as implemented by the U.S. Geological Survey, is to use look-up tables that pre-calculate the distance correlation between the point-source and finite-fault for the area of interest. As proposed by Bommer and Akkar [2012] a more pragmatic solution for using consistent distance metrics in hazard calculations would be to develop GMPEs in pairs; one that uses an extended-source distance metric for PSHA applications to fault sources and the other that is based on either  $R_{\text{epi}}$  or  $R_{\text{hyp}}$  to properly consider the contribution of areal source zones to overall hazard. This approach has begun to be adopted in the recently developed predictive models [Bindi *et al*, 2010; for  $R_{\text{epi}}$  and  $R_{\text{JB}}$ ] that can be considered as the future practice for producing consistent GMPEs.

Challenges in using the predictive models of different distance measures can also emerge while testing their suitability for the seismic hazard analysis of a given seismotectonic region. If the metadata information of the database that is compiled for the region in question contains reliable information on the distance metrics used by the candidate GMPEs, each model can be tested using its original distance definition. This approach was implemented in the SHARE [1] project while testing the candidate GMPEs for different seismotectonic regions in Europe [Delavaud *et al*, 2012]. Each candidate ground-motion model was tested using the comprehensive SHARE strong-motion database [Yenier *et al*, 2010] compiled for the particular needs of the project. If, on the other hand, the database lacks complete information about the distance measures used by the candidate GMPEs then one of the above distance conversion relations should be employed for obtaining the missing distance data. If such distance conversions are held before testing, there may be some uncertainty and this may decrease the reliability of the testing results. Figures 4.3 to 4.5 illustrate this fact by plotting the relations between  $R_{\text{JB}}$  and the other three distance metrics (i.e.,  $R_{\text{epi}}$ ,  $R_{\text{hyp}}$  and  $R_{\text{rup}}$ ) using the strike-slip recordings of the SHARE strong-motion database. Each figure consists of three panels that show the variation between the chosen distance pair for different magnitude intervals ( $5 \leq M_w < 6$ ,  $6 \leq M_w < 7$  and  $M_w \geq 7$ ). The plots also present the average relations between each distance pair using the Scherbaum *et al* [2004] expressions. The average Scherbaum *et al* [2004] trends plotted in each panel show the variations corresponding to the upper and lower magnitude bounds of the subject magnitude interval. The diagonal lines in each panel show that empirical  $R_{\text{JB}}$  values are smaller than the corresponding values of other distance measures, which is consistent in terms of theory.

From Figure 4.3 it can be inferred that an increase in magnitude inflates the dispersion about the mean Scherbaum *et al* [2004] curves for the empirical  $R_{\text{JB}}$  vs.  $R_{\text{epi}}$  relations. This trend is expected because the down-dip width and length of the rupture area in larger events become significant, which results in larger uncertainty in the exact location of the earthquake, that cannot be accounted for by the theoretical distance relations even if they are physically justifiable. Consequently, considerable divergence occurs between  $R_{\text{JB}}$  (finite source) and  $R_{\text{epi}}$  (point-source) distance metrics. The scatter between the empirical  $R_{\text{JB}}$  vs.  $R_{\text{hyp}}$  data and the mean Scherbaum *et al* [2004] curves (Figure 4.4) is even more evident regardless of the magnitude interval. This observation is also expected because  $R_{\text{hyp}}$  inherently considers the depth term whereas  $R_{\text{JB}}$  is a horizontal distance measure between the source and the site. Similar comparisons for  $R_{\text{JB}}$  vs.  $R_{\text{rup}}$  (Figure 4.5) indicate that scatter between the empirical data and the theoretical Scherbaum *et al* [2004] curve is prominent for small magnitude events. The differences become less significant for large magnitude cases (i.e.,  $M_w \geq 7$ ). Discrepancy between the empirical  $R_{\text{JB}}$  vs.  $R_{\text{rup}}$  data and the mean Scherbaum *et al* [2004] curves diminish considerably at distances larger than 20 km for events  $5 \leq M_w < 7$ . Empirical  $R_{\text{JB}}$  vs.  $R_{\text{rup}}$  data and mean Scherbaum *et al* [2004] seem to converge at distances larger than 10 km for events of moment magnitudes greater than 7. Both  $R_{\text{JB}}$  and  $R_{\text{rup}}$  are extended source distance measures and as the site is located further away from the source the depth term that is used in  $R_{\text{rup}}$  loses its significance, which may speculatively explain the convergence between these two distance metrics at larger distances. These

observations suggest that if the compiled database is not complete in distance during the testing of a set of GMPEs, the GMPEs that use  $R_{JB}$  or  $R_{rup}$  should be preferred since distance conversions between extended-source distance metrics seem to bring lesser uncertainty, particular for distances greater than 20 km.

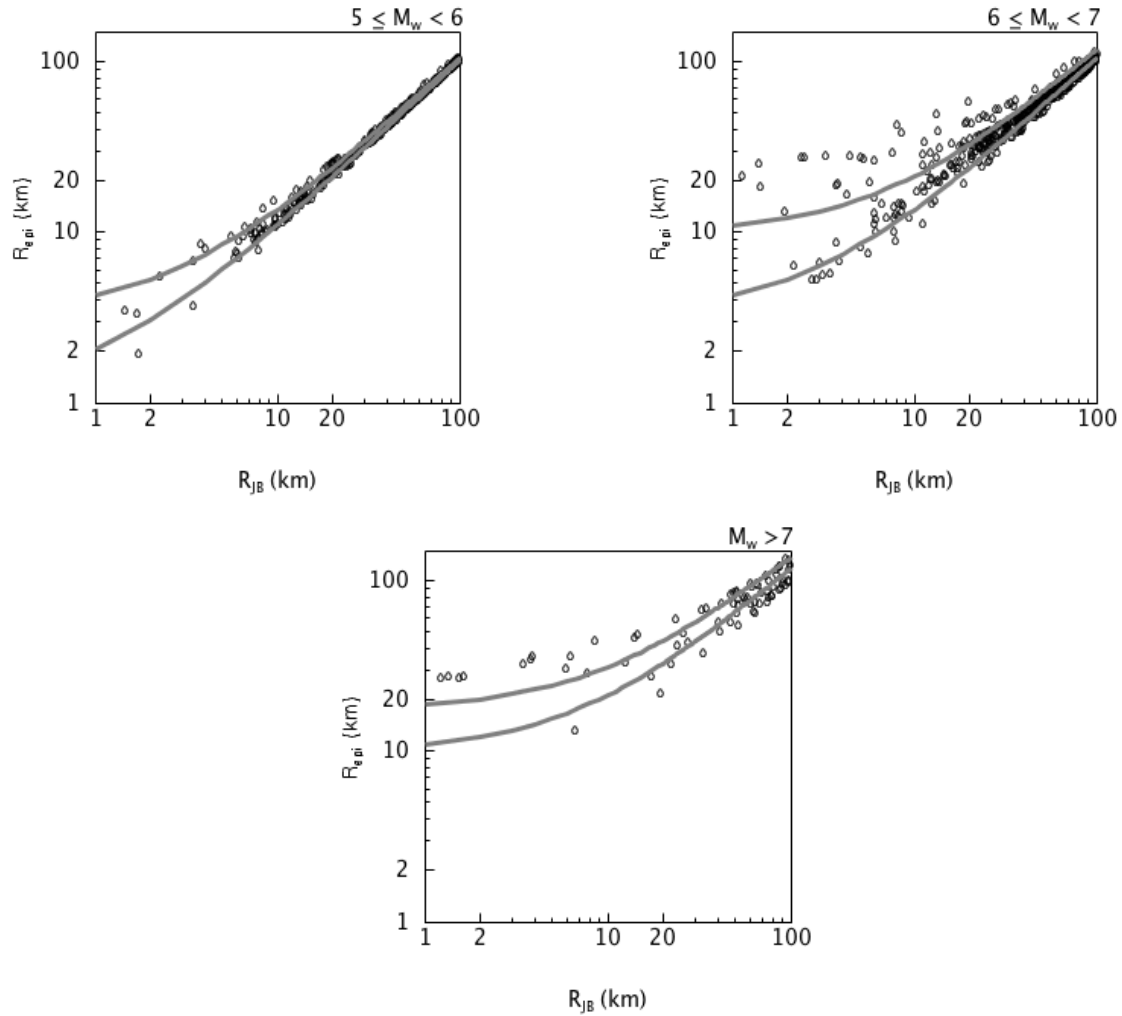


**Figure 4.3:**  $R_{epi}$  vs.  $R_{JB}$  scatters in strike-slip style-of-faulting events for different magnitude intervals and their comparisons with the average trends computed from the Scherbaum *et al* [2004] relationships. The data are gathered from the recently compiled SHARE ground-motion databank [Yenier *et al*, 2010].

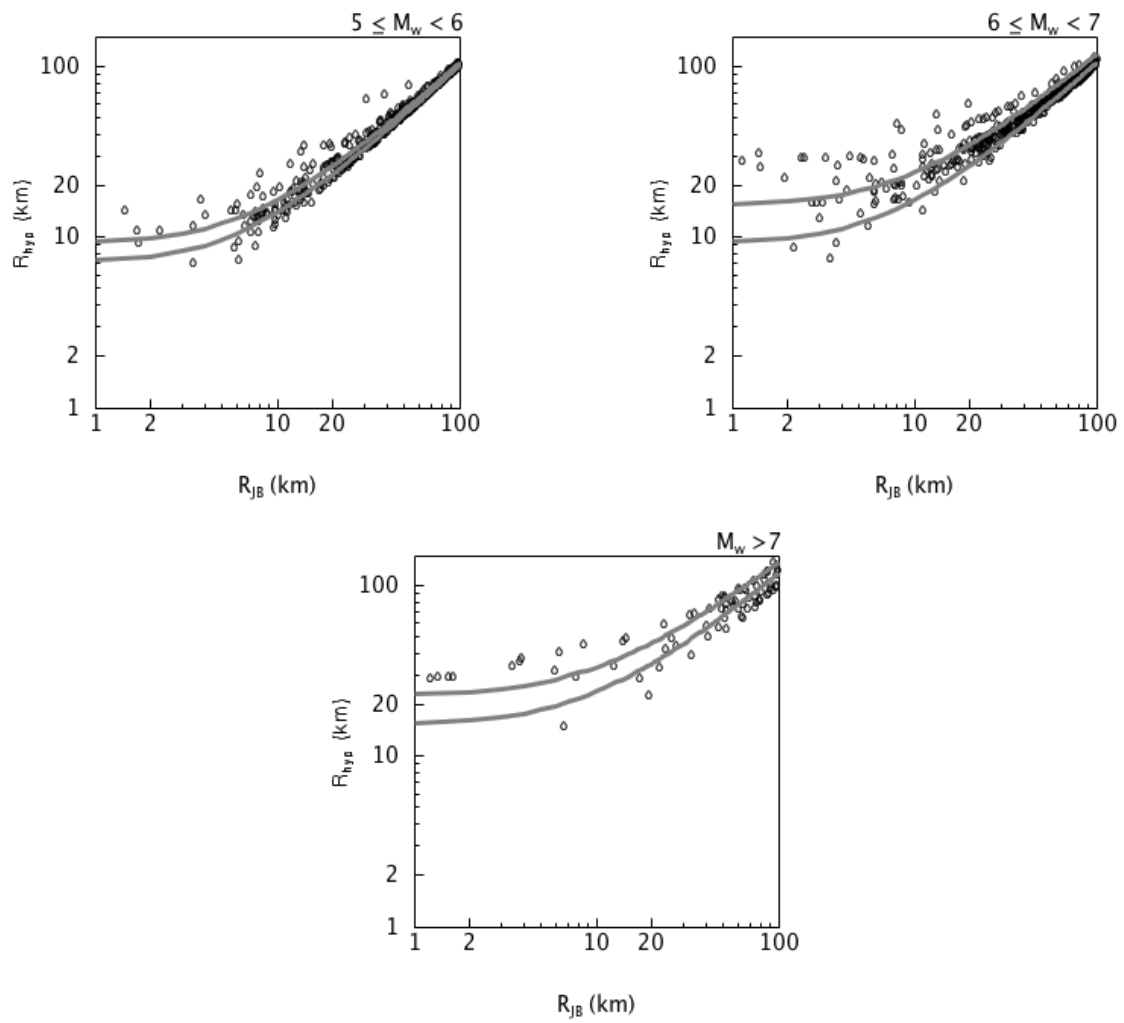


**Figure 4.4** Same as Figure 4.3 but for  $R_{hyp}$  vs.  $R_{JB}$ .

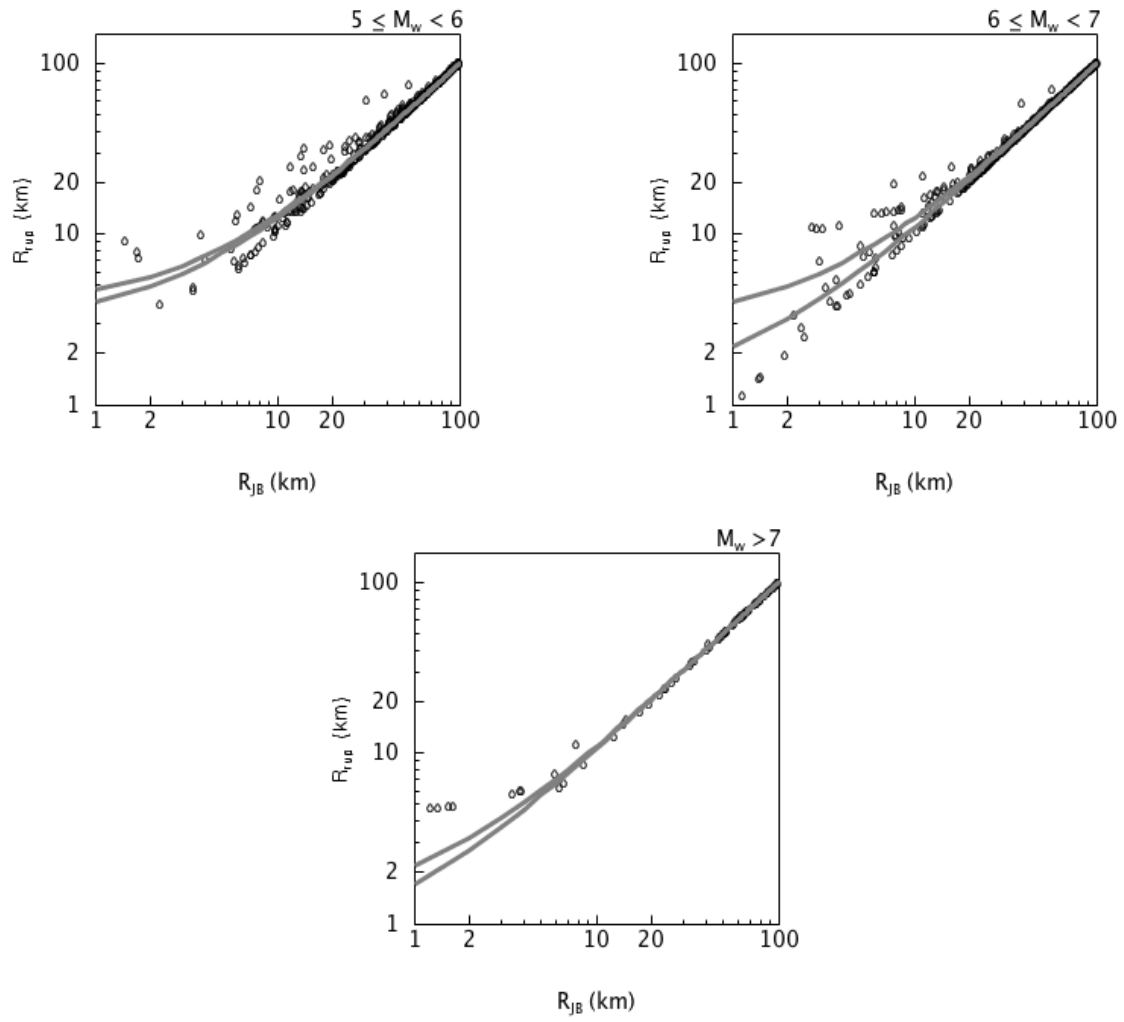


**Figure 4.5** Same as Figure 4.4 but for  $R_{rup}$  vs.  $R_{jB}$ .

## 5 Consideration of Style of Faulting

Style-of-faulting (SoF) describes the variation of ground-motion amplitudes for different fault mechanisms. The current improvements in strong-motion databases in terms of event information have increased the use of SoF as an independent estimator parameter in GMPEs during the last decade. However, the number of GMPEs that fully addresses the SoF effect on the ground-motion amplitudes is still limited. For example, of the 188 worldwide ground-motion models that estimate spectral ordinates [Douglas, 2011], only 23 GMPEs clearly distinguish the spectral amplitude difference between normal, strike-slip and reverse/thrust rupture mechanisms<sup>3</sup> for active shallow crustal regions (there are a number of models that group earthquakes with normal or strike-slip mechanisms in a single class and model the difference in amplitudes between this class and reverse/thrust events). Some of these ground-motion models also consider the footwall and hanging wall effects on the variation of ground-motion amplitudes for dipping faults. These GMPEs are almost exclusively derived from global strong-motion databases because SoF information in such datasets is more complete and reliable than most local datasets. The local ground-motion models, in cases when they consider the style-of-faulting effects, generally focus on one or two styles-of-faulting based on the specific tectonic structure of the considered region. The number of GMPEs that account for different rupture mechanisms in subduction regions is even smaller. Douglas [2011] lists less than 10 GMPEs that differentiate ground-motion amplitudes between interface and intraslab events. Depending on the complexity of tectonics in the considered region as well as the extent of the strong-motion dataset, some GMPEs that are derived for subduction zones also consider crustal earthquakes.

For crustal events, the SoF factors are typically between -0.2 and 0.2 natural log units. This is a small term relative to the aleatory standard deviation of about 0.6 to 0.7 natural log units. As a result, the inclusion of SoF as an additional estimator parameter in GMPEs only slightly reduces the total aleatory variability [Boore et al, 1997; Boore and Atkinson, 2008]. On the other hand, if the hazard in a region is dominated by a single style-of-faulting, then  $\pm 0.2$  on the median can lead to factors of 2–3 differences in the hazard so the effects can be significant.

This chapter discusses the alternative schemes used for the classification of SoF and the significance of database distribution on the evaluation of SoF scaling. The chapter concludes with a suggested strategy for the consideration of SoF in the predictive models that, in turn, leads to physically justifiable (consistent) results in PSHA.

---

<sup>3</sup> Although normal, strike-slip and reverse/thrust fault mechanisms are the main styles-of-faulting, the combination of strike-slip faulting with either reverse or normal faulting is defined as oblique faulting. For such cases the larger component of faulting is expressed first.

## 5.1 Challenges Styles of Faulting Classification Approaches

The style-of-faulting can be determined from the tectonic configuration and crustal stresses, fault-plane solutions reported by seismic agencies and centroid moment tensor (CMT) solutions. The latter two options are of main use for ground-motion models as they not only provide the necessary information for classifying the faults but also help define the geometry of the fault plane for calculating the extended-source distance measures. The information provided by these two options is either the rake (slip) angle or the plunge of the P, T and B axes for grouping different rupture mechanisms. The majority of model developers categorize the SoF using the rake angle information. Table 5.1 lists some of the SoF classifications that use rake angle intervals as well as the plunges of the P, T and B axes. The SoF classifications that are based on this information vary from one scheme to the other indicating that there is no well-accepted definition for each of these types of faulting mechanisms. Figure 5.1 shows the variation of normal to strike-slip and reverse to strike-slip spectral ordinate ratios that are computed from the GMPEs that use the SoF classifications listed in Table 5.1. The differences in the SoF factors shown in Figure 5.1 are not mainly due to the different classification schemes. Rather, there is a trade-off between SoF scaling and depth scaling. For example, in the NGA database, the SoF is correlated with depth as there are more buried reverse earthquakes than buried strike-slip earthquakes. Those GMPEs that include a depth term will tend to have a smaller SoF term.

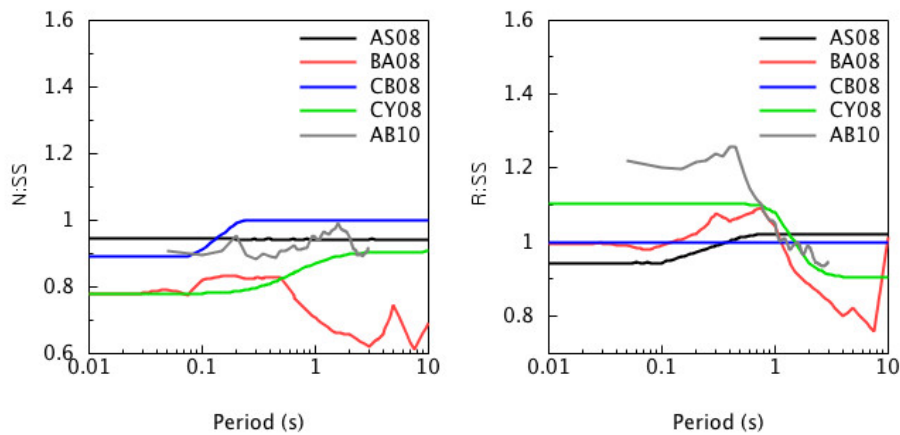


**Figure 5.1** Given a set of GMPEs, the normal and reverse spectral ordinates for a rock site ( $V_{s30} = 760$  m/sec) that are normalized by the corresponding strike-slip spectral ordinates (i.e., N:SS and R:SS, respectively). The magnitude of scenario earthquake is Mw 7. The fault rupture is assumed to emerge at the surface. The abbreviations AS08, BA08, CB08, CY08 and AB10 that are given in the graph legend refer to Abrahamson and Silva [2008], Boore and Atkinson [2008], Campbell and Bozorgnia [2008], Chiou and Youngs [2008] and Akkar and Bommer [2010], respectively.

In general the differences in rake angle schemes do not result in inconsistent SoF classification. However, Bommer *et al* [2003] and Boore and Atkinson [2007] indicated that a SoF classification that is based on rake angle may not be practical for some cases because, unless the ruptured plane is known, the two nodal planes obtained from the fault-plane or CMT solutions may give different fault mechanisms, leading to ambiguity in the SoF classification. Using classification schemes that employ the plunges of the P, T and B axes does not lead to such complexities in the SoF classification. This approach does not use the rake angles of focal planes, thus, it leads to a unique SoF classification of earthquakes. The proposed plunge angles of Frolich and Apperson [1992] would classify some of the earthquakes as “odd” that may roughly correspond to those events which cannot be unambiguously classified through rake angle definitions due to the missing ruptured

plane information in the fault-plane solutions [Bommer *et al*, 2003]. Boore and Atkinson [2007] used a slightly modified version of the plunge angles proposed in Zoback [1992] to map them into fault types, while developing their ground-motion prediction model. This simplified classification scheme does not use the plunge of the B axis and rarely fails to classify the earthquakes into one of the fault mechanisms.

The discussions in the above paragraphs focus on the classification of fault types for crustal earthquakes. The SoF classification for subduction earthquakes requires the consideration of depth. The tectonic deformation in subduction regions results in crustal as well as interface and intraslab subduction earthquakes. The crustal thickness (about 25-30 km in most tectonically active regions) is considered as the bounding depth for crustal earthquakes. The subduction slab earthquakes occur at greater depths (e.g., over 50 km for Japan according to Zhao *et al*, [2006]). The depth range of interface earthquakes is generally in between the depth ranges of the crustal and intraslab subduction earthquakes, however, the focal depths of each of these earthquake types can overlap within a given region. Subduction interface earthquakes are often classified with one of the nodal planes parallel to the subduction interface. The focal mechanism of interface earthquakes is often thrust and it is generally defined by the rake angle information [Zhao *et al*, 1996; Sadigh *et al*, 1997]. Subduction slab events often have a strike-slip or normal focal mechanism and the current approach is to use rake angle information for their classification.

## 5.2 Influence of Database Distribution on Style of Faulting-based Ground Motion Amplitudes

The distribution of recordings in a database that are used in the derivation of GMPEs can also play a role in the estimated ground-motion amplitudes for different rupture mechanisms. This fact is illustrated using a pan-European ground-motion dataset that contains shallow crustal recordings of  $4 \leq M_w < 7$  and  $R_{jb} \leq 200$  km. Successive random-effects regression analyses were done for different cases (subsets of the original dataset) to compare the estimated spectral ratios for reverse, normal and strike-slip SoF in each case. The cases are indicated below:

- Original dataset (Normal: 604, Strike-slip: 383, Reverse: 167 recordings)
- Excluding singly-recorded events from the entire dataset (Normal: 522, Strike-slip: 319, Reverse: 144 recordings)
- Excluding singly-recorded events as well as removing events with less than 3 recordings for  $M_w \leq 5$  (Normal: 498, Strike-slip: 265, Reverse: 121 recordings).

Figure 5.2 shows the magnitude vs. distance distributions of the datasets that are used in the regression analyses in terms of SoF. Figure 5.3 displays the normal to strike-slip (N:SS) and reverse to strike-slip (R:SS) spectral ratios obtained from the above 3 cases. In all cases the same functional form is used in order not to introduce any bias in the comparisons. Since the SoF classification for the considered datasets is the same, the ambiguity due to different SoF classification definitions does not come into the picture in these comparisons. The recordings are modified for  $V_{s30} = 760$  m/s using a site function that is derived from the same dataset [Sandikkaya *et al*, 2012]. The scatter plots in Figure 5.2 depict that the data scatter does not show a large change for the studied cases. However, the normalized spectral ordinates given in Figure 5.3 show considerable variations, in particular, between cases (a) and (c). When the left-hand panels in Figures 5.1 and 5.3 are compared, one can immediately observe that N:SS ratios larger than 1 are counterintuitive suggesting that the SoF coefficients obtained from the regression analysis of case (a) are biased towards estimating unexpectedly large ground motions for normal rupture mechanism. The studies investigating the

N:SS ratios generally conclude that normal-faulting events produce lower ground motions with respect to strike-slip earthquakes (see detailed discussions in Bommer *et al.*, [2003]). The right-hand panels on Figures 5.1 and 5.3 indicate that R:SS ratios for cases (a) and (b) are considerably larger than those that are computed from the chosen GMPEs. Although there are particular reverse-faulting events that resulted in unexpectedly large ground motions (e.g., Coalinga aftershock sequence, the 1987 Whittier Narrows and 1994 Northridge earthquakes that occurred in California and are not included in the dataset used here) with respect to the strike-slip events, the values obtained from such cases should be interpreted with some caution because the median R:SS ratios such as those given in Figure 5.1 should reflect the generally expected amplitude differences between the reverse and strike-slip ground-motion amplitudes. The agreement between the R:SS trends of GMPEs and case (c) is better. The R:SS ratios presented in case (c) are also consistent with the findings in the literature that suggest an R:SS ratio ranging between 1.0 and 1.2 for high-frequency ground-motion components. These observations suggest that the singly-recorded events in the original pan-European dataset as well the small magnitude (i.e.  $M_w < 5$ ) events with less than 3 recordings introduce bias in the SoF regression coefficients and should be avoided in order to estimate physically justifiable ground-motion amplitudes in terms of SoF.

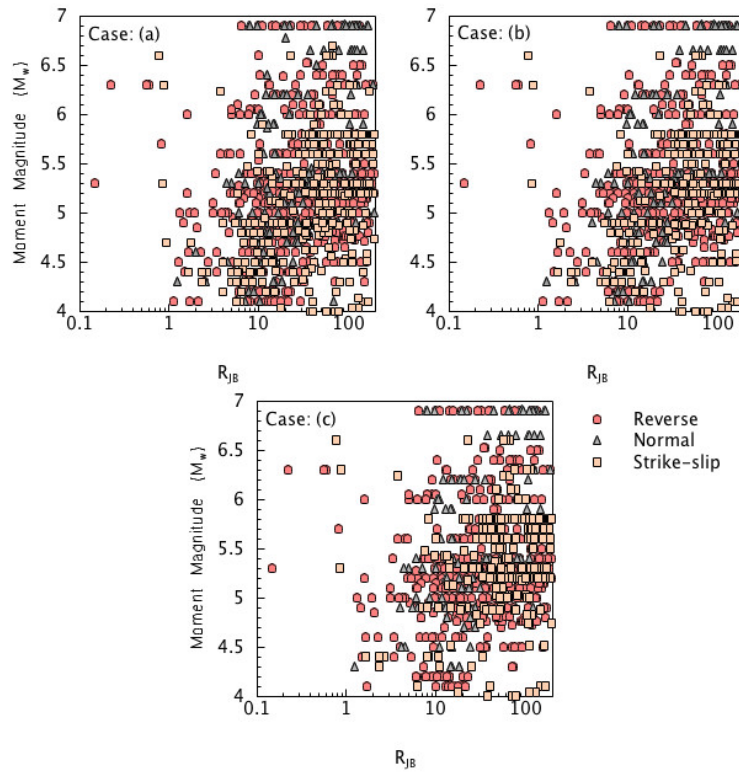


**Figure 5.2** Magnitude ( $M_w$ ) vs. distance ( $R_{JB}$ ) scatter of the datasets used for the case studies.



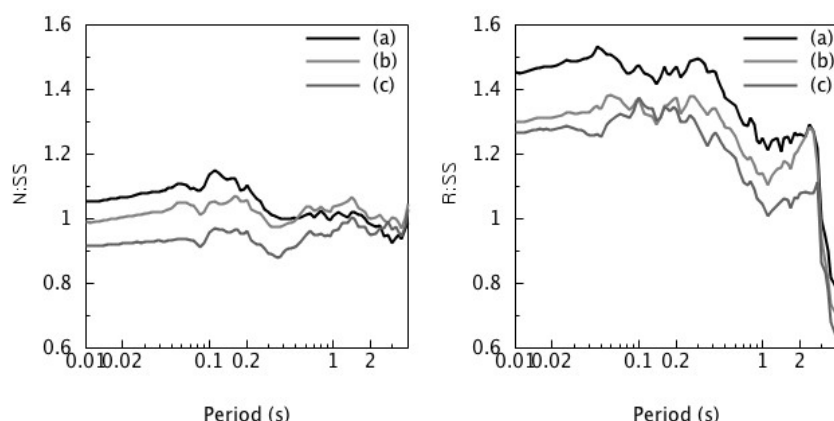


**Figure 5.3** Normal to strike-slip (N:SS) and reverse to strike-slip spectral ordinate ratios for the three cases that are studied for investigating the sensitivity of database distribution in the estimated ground-motion amplitudes for different SoF. The sudden drop in R:SS after  $T = 2$  sec can be due to sparse data and should be considered with caution.

### 5.3 The Issue of Providing Consistence in Style of Faulting for PSHA Computations

The consideration of style-of-faulting as a predictive parameter in GMPEs is now common. As is often the case for empirical models, there can be strong trade-offs between the SoF factor and other predictive parameters such as depth. Reliable depth information is important for identifying the rupture mechanisms as well as different tectonic regimes for subduction zones. Depth and focal mechanism or centroid moment tensor (CMT) information provides a good way to distinguish crustal, interface and intraslab subduction earthquakes. The classification schemes used for mapping the earthquakes into different fault mechanisms and the database distribution also affect the estimated ground-motion amplitudes for different types of faulting. Using the plunge of the P, T and B axes seems to be a reliable way of classifying different styles-of-faulting although rake angle schemes yield consistent SoF classifications for many cases. Thus, use of plunge of P, T and B axes should be verified with the rake angle intervals as implemented by Boore and Atkinson [2007] in order to reduce the number of unclassified earthquakes in terms of SoF. The reliability of event information in the dataset that is used for developing the ground-motion model is also important.

Currently most of the global GMPEs and a few local ones address SoF. The ground-motion models that include the SoF estimator parameters should be preferred in PSHA as long as they address correlations with other parameters that can also explain the observations and are proven to be efficient and accurate for the considered seismic region (see Task 2 report for the pre-selection of GMPEs for hazard analysis). There are proposed schemes to incorporate the style-of-faulting into GMPEs that either consider only one fault mechanism or are independent of rupture mechanisms. Bommer *et al* [2003] propose a scheme to account for SoF in such GMPEs for improved PSHA. Unless there are compelling reasons for using such adjusted GMPEs in the hazard analysis, the use of methodologies that externally adjust the estimated ground-motion amplitudes for SoF effects should be avoided. Such manipulations would increase the uncertainty in the estimated ground motions.

**Table 5.1** Classification schemes for style-of-faulting (modified from Bommer *et al* [2003]).

Authors	N	SS	R/T	Other
Abrahamson and Silva [2008]	$-120 \leq \lambda \leq -60$	$-60 < \lambda < 30$ $-120 < \lambda < 150$	$30 \leq \lambda \leq 150$	
Akkar and Bommer [2010]	$\delta_p > 60$	$\delta_B > 60$	$\delta_T > 50$	All other combinations are described using rake angle definitions of Sadigh <i>et al</i> [1997]
Boore and Atkinson [2008]	$\delta_p > 40$ and $\delta_T \leq 40$	$\delta_p \leq 40$ and $\delta_T \leq 40$	$\delta_p \leq 40$ and $\delta_T > 40$	All other combinations are described as undefined.
Campbell and Bozorgnia [2008]	$-150 \leq \lambda \leq -30$	$-30 < \lambda < 30$ $-150 < \lambda < 150$	$30 \leq \lambda \leq 150$	
Chiou and Youngs [2008]	$-120 \leq \lambda \leq -60$	$-60 < \lambda < 30$ $-120 < \lambda < 150$	$30 \leq \lambda \leq 150$	
Boore <i>et al</i> [1997]	$-150 \leq \lambda \leq -30$	$-30 < \lambda < 30$ $-150 < \lambda < 150$	$30 \leq \lambda \leq 150$	
Campbell [1997]	$-157.5 \leq \lambda < -22.5$	$-22.5 < \lambda < 22.5$ $-157.5 < \lambda < 157.5$	$22.5 \leq \lambda \leq 157.5$ and $\delta \geq 45$	
Sadigh <i>et al</i> [1997]	$-135 \leq \lambda \leq 45$	$-45 < \lambda < 45$ $-135 < \lambda < 135$	$45 \leq \lambda \leq 135$	
Frohlich and Apperson [1992]	$\delta_p > 60$	$\delta_B > 60$	$\delta_T > 50$	All other combinations are called "odd".

N, SS, R and T refer to normal, strike-slip, reverse and thrust rupture mechanisms, respectively;  $\lambda$  is rake angle;  $\delta_p$ ,  $\delta_B$ ,  $\delta_T$  are the plunge angles of P, B, and T axes, respectively.

## 6 Consideration of Near-Fault Effects

An earthquake is a shear dislocation that begins at a point on a fault and spreads at a velocity that is almost as large as the shear-wave velocity. The propagation of fault rupture toward a site at a velocity close to the shear-wave velocity causes most of the seismic energy from the rupture to arrive in a single large pulse of motion that occurs at the beginning of the record [Somerville *et al*, 1997]. This pulse of motion represents the cumulative effect of almost all of the seismic radiation from the fault. The radiation pattern of the shear dislocation on the fault causes this large pulse of motion to be oriented in the direction perpendicular to the fault plane, causing the strike-normal component of ground motion to be larger than the strike-parallel component at periods longer than about 0.5 seconds. To accurately characterize near-fault ground motions, it is therefore necessary to specify separate response spectra and time histories for the strike-normal and strike-parallel components of ground motion. Thus, supplementary ground-motion models that account for such variations of ground-motion amplitude in the vicinity of faults are required to modify the ground-motion estimations computed from generic models. (The term “generic model” refers to ground-motion models that do not directly address near-fault effects). These models should consider the location of a site with respect to the fault rupture and other parameters (e.g., hanging-wall effect for dipping faults and source directivity) to capture near-fault effects on the ground-motion amplitudes. Near-fault effects are often referred to as directivity and/or directionality effects. In addition, fault-rupture dynamics that result in trapped waves in the wedge between the fault plane and the ground surface is also influential in the variation of ground-motion amplitudes in the vicinity of causative fault [e.g., Marra *et al*, 2000].

### 6.1 Directivity

Directivity effects cause variations in response spectral accelerations that are not accounted for fully by standard ground-motion prediction models. Directivity effects generally increase spectral accelerations at locations where the rupture has propagated towards the site of interest, for periods longer than approximately 0.5 s. At locations where the rupture has propagated away from the site, spectral accelerations generally decrease. Forward-directivity effects are manifested in the presence of a short-duration velocity pulse, which is not modeled by most ground motion prediction models. Because the directivity effect depends upon rupture direction, additional predictor parameters are needed to account for this effect. Most directivity models use a description of the amount of the rupture that has ruptured towards the site of interest, and also the total length of overall rupture. Directivity models require the hypocenter location to be specified, and the entire extent of rupture to be specified, so point-source descriptions of earthquakes or descriptions that do not specify a hypocenter are not suitable for directivity predictions. Directivity models also need to address the dependence of directivity effects on faulting mechanism

The first directivity model was developed by Somerville *et al* [1997] based on analysis of near-fault strong-motion recordings. This model provides separate predictions of the strike-normal and strike-parallel components of motion, and was later modified by Abrahamson [2000] for strike-slip earthquakes. These are currently the most widely used models for hazard calculations because they use simple parameters that are

easy to implement. There are also more complicated models to implement, such as the ones developed by Rowshandel [2006 and 2010] within the NGA project, or the ones that are currently under study within the context of the NGA-West2 [4] project. The models proposed by Rowshandel [2006 and 2010] are capable of handling every type of rupture direction because they generalize the directivity predictors of Somerville *et al* [1997] by applying a surface integral over the fault for every receiver location. The Rowshandel [2010] model assumes a distance-dependency for the directivity factors, whose values tend to decay rapidly at magnitudes around 6. However, the Rowshandel [2006] model, like the one from Somerville *et al* [1997], does not include such distance-dependency that results in relatively large directivity effects at large distances from the source.

The Somerville *et al* [1997] model includes differences between the strike-normal and strike-parallel components of motion. The ratio of strike-normal to average horizontal motions is found to depend primarily on earthquake magnitude and rupture distance, while the dependencies on faulting mechanism and site category is found not to be practically significant. The ratio of strike-normal to average horizontal motions is found to be period-dependent, and becomes significant for periods greater than 0.6 s, indicating a transition from incoherent source radiation and wave propagation conditions at short periods to coherent source radiation and wave propagation conditions at long periods.

Based both on analysis of ground motion simulations and the database of recorded ground motions developed for the NGA project, Spudich and Chiou [2008] developed a new physically-based directivity model using isochrone theory. Their model is built on a more rigorous theoretical basis and an updated, expanded strong-motion database, and provides an improved characterization of directivity over the earlier models. Although it can be applied to the NGA GMPEs, it would likely be difficult to apply to other models in the GEM hazard calculations. The Spudich and Chiou [2008] directivity model currently does not address differences between strike-normal and strike-parallel components.

In the Somerville *et al* [1997] model, rupture directivity is modeled as a broadband effect, which increases with increasing period beyond 0.6 s, and increases with earthquake magnitude. However, near-fault recordings from recent earthquakes indicate that the rupture directivity pulse is a narrow band pulse whose period increases with magnitude, as expected from theory [Somerville, 2003]. This magnitude dependence of the pulse period causes the response spectrum to have a peak whose period increases with magnitude, such that the near-fault response spectral accelerations from moderate magnitude earthquakes may exceed those of larger earthquakes at intermediate periods (around 1 second). However, a complete narrow band representation of near-fault response spectra, analogous to the broadband model of Somerville *et al* [1997], has not yet been developed.

Near fault ground motions containing forward rupture directivity may be simple enough to be represented by simple time domain pulses, thus simplifying the specification of ground motion time histories for use in structural response analyses. Preliminary equations relating the period of the pulse to the earthquake magnitude, and the effective velocity of the pulse to the earthquake magnitude and distance, have been developed by Somerville [2003] and other investigators [e.g., Bray and Rodriguez-Marek, 2004; Alavi and Krawinkler, 2004]. For large surface faulting earthquakes (e.g., the  $M_w$  7.6 Chi-Chi earthquake), the value of the pulse period may also be affected by the large permanent displacements accompanying the fault rupture, and limitations in the ability of standard record processing techniques to address the effects of permanent displacements on the velocity time history of a record. Although considerable differences exist between the predictions of different models, all of the correlations show a similar trend of pulse period increasing with earthquake magnitude.

Directivity effects induce systematic spatial variations of duration in near-fault ground motions. In general, the time history is compressed in time in the forward-directivity region, especially on the strike-normal component, while in the backward-directivity region the time history is elongated in time. Engineers tend to question the brief duration of forward directivity near-fault ground motions that are provided to them for design. This tendency should be resisted, because brief durations are a predictable feature of near-fault ground motions unless there is the potential for multiple rupture episodes on a complex fault system, or there is the potential for basin response to generate long durations. Somerville *et al* [1997] proposed an empirical model using directivity predictors like those used to model the response spectrum. The model predicts that, at the locations where maximum directivity effects are obtained, the ground motion duration is about 0.55 times the average duration for both strike-slip and reverse faulting; whereas at locations having the minimum directivity effects, the ground motion duration is about 2.1 times the average duration for dip-slip faulting, and 1.6 times the average duration for strike-slip faulting.

## 6.2 Directionality

Most ground-motion prediction models are for the average (“geometric mean”) of the response spectra of two horizontal components. In some cases it may be of greater interest to know the maximum spectral value, over all possible directions, of spectral acceleration at a given period. Popular existing models for making such a “maximum direction” prediction by modifying a basic GMPE are those by Beyer and Bommer [2006], Watson-Lamprey and Boore [2007] and Boore [2010]. Loosely speaking, the maximum-direction spectral value will be about 1.2 times the geometric mean value at short periods, and 1.3 times the geometric mean value at long periods. The standard deviation of maximum-direction spectral value predictions is larger than that for geometric mean predictions.



## 7 Consideration of Other Important Parameters such as Basin Effects, Depth to Top-of-Rupture, $Z_{1.0}$ , $Z_{2.5}$ , Nonlinear Site Effects and $V_{S30}$ - $\kappa$ Correlations

Many additional parameters have been shown to be important in the reliable estimation of ground motion and should be considered in the ground-motion model as long as there are reliable metadata characterizing such effects. For instance, parameters such as  $Z_{TOR}$  (depth to top-of-rupture),  $Z_{1.0}$  and  $Z_{2.5}$  (depth from the ground surface at which shear-wave velocity attains values of 1.0 km/sec and 2.5 km/sec, respectively) are only available in a few databases for a limited number of sites. It may still not be feasible for many model developers to consider them in ground-motion models. Also the parameter  $R_x$ , the shortest horizontal distance to the top edge of rupture measured perpendicular to the strike (site coordinate), has an important role when considering hanging-wall effects. A recent paper by Kaklamanos *et al* [2011] evaluates the NGA models in the R and Fortran computer languages, and proposes default values for fault dips,  $Z_{TOR}$  and other NGA parameters when they are unknown [also see Appendix A of Petersen *et al* 2008]. However, care should be taken in evaluating how sigma increases when considering these “default” values.

Nonlinear site effects are currently estimated by using the average shear-wave velocity in the upper 30 m soil profile ( $V_{S30}$ ). Unfortunately measured  $V_{S30}$  values are still rare in many strong-motion databases and for many regions current ground-motion models consider generic soil classes to model site effects. Task 1.b report Stewart *et al*, 2011] will provide guidance on how to evaluate  $V_{S30}$  values, as well as provide default site conditions when they are unknown for a given site.

The average  $V_{S30}$  and  $\kappa$  (high-frequency filtering commonly considered to be related to near-surface attenuation) on rock can significantly affect short-period response spectral ordinates. GMPEs developed for different parts of the world have used different rock definitions and consequently require calibration to a specific rock definition. This is reasonably straightforward for models, such as the NGA models, which treat  $V_{S30}$  as a variable.  $V_{S30}$  and  $\kappa$  are considered to be strongly correlated [e.g., Silva *et al*, 1996; Van Houtte *et al*, 2011]. Therefore a coupled  $V_{S30}$ - $\kappa$  correlation, despite large uncertainties, can be used to calibrate GMPEs for a specific rock definition [Van Houtte *et al*, 2011]. . Van Houtte *et al* [2011] considered two types of rock (generic rock:  $V_{S30} = 800\text{m/s}$ ,  $\kappa = 0.03\text{ s}$  for active regions; and hard rock:  $V_{S30} = 2800\text{m/s}$ ,  $\kappa = 0.01\text{ s}$  for stable regions) while making such a calibration for SHARE. We note that such  $V_{S30}$  vs.  $\kappa$  calibrations can be done for sites having reliable shear-wave velocity information. In the context of this project such relationships are encouraged to provide guidance in hazard analysis to describe rock conditions in different parts of the world.





## 8 Consideration of Dispersion about the Median

Regardless of the level of complexity in GMPEs, the idealizations imposed by these models result in departures between the observed and estimated ground-motion parameters and this dispersion (unexplained component of the ground-motion model) is described by the standard deviation (sigma) associated with the predictive model. Although sigma is usually interpreted as describing the aleatory uncertainty of ground motions, it can also convey information on the epistemic (modeling) component of uncertainty due to differences in opinion on such factors as the functional form, what parameters should be included, and what data should be included in the ground-motion model. The logarithmic behavior of the predictive models [Campbell, 1985; Douglas and Smit, 2001] indicate that the dependent ground-motion parameter is an exponential function of sigma, thus its value has a significant impact on the seismic hazard analysis, in particular, at low annual exceedance rates [Bommer and Abrahamson, 2006]. Therefore research efforts should focus on a better understanding of the nature of sigma and its estimation. The text in this section summarizes the important components used in the derivation of GMPEs that control the variation of sigma, and discusses current as well as future considerations for its estimation or reduction in its level. More detailed discussions on this topic exist in Strasser *et al* [2009] and other references cited here.

The accuracy of the predicted ground-motion parameters can affect the value of sigma, which emphasizes the importance of the selection and processing of the strong-motion data that are used in the regression analysis [Strasser *et al*, 2009]. The significance of data processing of ground-motion parameters is discussed in the following section. Censoring the low-quality strong-motion data may positively influence the goodness-of-fit of the regression analysis. However, this should be done carefully because conservative down-sampling of data may lead to misrepresentation of the tails of the ground-motion distribution that, essentially, can misrepresent the variability in the estimated ground-motion parameter. Poorly digitized recordings, low quality data due to instrument malfunction and late-triggered data can be classified as defective and removed from the ground-motion dataset.

The choice of horizontal component of the ground motion adopted in the ground-motion model will also have an effect on the sigma value because certain horizontal component definitions show more variability than the others [Beyer and Bommer, 2006; Watson-Lamprey and Boore, 2007]. Studies conducted by Boore *et al* [1997], Beyer and Bommer [2006] and Campbell and Bozorgnia [2007] suggests that the random component definition introduces a larger sigma compared to other horizontal component definitions.

The reliability of metadata information of the strong-motion database will also contribute to sigma. The measurement errors in magnitude affect the inter-event variability [Rhoades, 1997]. Abrahamson and Silva [2007, 2008] also showed that consideration of measurement errors in magnitude and depth-to-top of rupture can have an impact in reducing the inter-event variability at long vibration periods. The significance of including style-of-faulting is found to be less important in reducing the sigma value [Boore and Atkinson, 2008].

The uneven distribution of ground motions in the databases must be addressed as much as possible in order to minimize the effect of correlations in the estimator parameters that in turn can have an influence in the calculation of sigma. Given the current limitations in strong-motion databases, equalizing their distribution is

difficult and consequently proper regression methodologies are needed for the reliable calculation of sigma. Two-stage regression techniques [Joyner and Boore, 1981] and distance-dependent weighting strategies [Campbell, 1981] were proposed in the derivation of predictive models but currently one-stage maximum likelihood techniques [Brillinger and Preisler, 1984; 1985; Abrahamson and Youngs, 1992; Joyner and Boore, 1993] that break sigma into inter- and intra-event components can be used more efficiently to prevent such correlations from biasing the regression. The intra-event variability can be decomposed into site-to-site and record-to-record variability as long as the data distribution is sufficient for such analysis. Recently, Jayaram and Baker [2010] emphasized the importance of spatial correlation between intra-event residuals for reducing the inter-event variability.

Recent ground-motion models consider the influence of estimator parameters on the dispersion about median estimations. Among the estimator parameters, magnitude has received the most attention of model developers because a decrease in magnitude seems to inflate sigma due to the errors involved in the magnitude determination of smaller events [Youngs *et al*, 1995; Douglas and Smit, 2001; Abrahamson and Silva, 2008; Chiou and Youngs, 2008]. However, other investigations found no significant evidence for the dependence of sigma on magnitude that can be the result of record- and event-based distribution of the strong-motion databases used in these studies. Other than the magnitude parameter, some studies find the dependence of sigma on distance and soil behavior. Midorikawa and Ohtake [2004] and Abrahamson and Silva [2007, 2008] indicate that sigma decreases as the site gets closer to the source. Increased nonlinear behavior of soil deposits also leads to a reduction in intra-event variability. A proper consideration of the influence of such parameters on sigma requires enhanced strong-motion databases and functional forms that can efficiently address the variation of different components of sigma against these estimator parameters.

Inclusion of additional predictor variables in the GMPEs can reduce the sigma but this effort requires well-constrained metadata information that would prevent additional uncertainty stemming from the inaccurate measurements of these parameters. Enhanced strong-motion databases with large numbers of recordings can also have a positive effect on reducing sigma. However, care should be taken while assembling these large ground-motion datasets because the collected data should be reliable and self-consistent. Otherwise, improper data can contaminate the entire strong-motion database instead of improving the distribution in terms of essential estimator parameters. This can eventually lead to unstable behavior of the ground-motion model that in turn can result in either a marginal reduction of sigma values or an increase in sigma, which is the least desirable phenomenon. Sigma can also be controlled by studying the behavior of its individual components of variability associated with a single event or a single station [e.g. Atkinson, 2006; Ordaz and Reyes, 1999; Rodriguez-Marek *et al*, 2011]. Such studies can be of use for site-specific hazard studies.

## 9 Consideration of Ground Motion Parameters (Intensity Measures)

### 9.1 Ground Motion Parameters (Intensity Measures) of Interest in this Project

Ground-motion models are the prime tools in seismic hazard analysis that provide the level of ground-motion demand on structural systems, which are used for the design and verification of structures against seismic action. Thus, the ground-motion intensity parameters of interest in the predictive models should primarily respond to the needs of the engineering community. Today both force-based and displacement-based design and seismic performance assessment codes/guidelines efficiently use the pseudo-spectral acceleration (PSA), spectral displacement (SD) as well as peak ground acceleration (PGA) and velocity (PGV) as the ground-motion intensity parameters. Since the use of these parameters in such engineering documents is expected to remain, at least, in the next decade the current and future GMPEs will continue to develop models for predicting them through enhanced functional forms associated with a more complete set of estimator parameters to better explain their intricate nature in terms of source, path and site effects. The compendium of GMPEs reported in Douglas [2011] indicates that there already are more than 285 predictive models for PGA and approximately 190 equations for predicting spectral ordinates that include PSA and SD. A significant proportion of these models also provide coefficients for the estimation of PGV.

### 9.2 Range of Reliable Spectral Ordinates and Signal Processing

Before using them in the derivation of GMPEs, the reliability of the ground-motion parameters that are calculated from the processed recordings needs to be considered. For example, the reliable estimation of long-period spectral ordinates is important for base-isolated structures as well as high-rise buildings and long-span bridges. Consistent short-period vertical spectral ordinates become essential for the derivation of horizontal-to-vertical spectral ratios as well as for the design of short-period machinery components mounted on building systems. Thus, data processing schemes must yield as much information as possible about the processed recordings without manipulating the actual frequency content of the data. Studies on data processing methods date back to the 1940s [Trifunac, 1971], but the most remarkable step forward in this field was the research conducted by Trifunac and his co-workers at Caltech for the compilation of the ground-breaking Blue Book series. The processing procedure of Trifunac [1973] involves instrument correction and removal of low-frequency noise via high-pass filtering and suggests using fixed filter cut-off frequencies to remove the noise-contaminated signal from the data. Iwan *et al* [1985] and Chen [1995] proposed baseline correction schemes alternative to digital filtering applications that aim to remove baseline shifts occurring during the strong ground shaking. Currently there are quite a few alternative baseline correction procedures [e.g., Boore, 2001; Akkar and Boore, 2009; Wu and Wu, 2007] in order to improve the ground velocity and displacement calculations obtained from the double integration of baseline corrected acceleration. Filtering procedures have also been modified since their first implementation [e.g., Sunder and Connor, 1982; Trifunac *et al* 1999; Trifunac and Todorovska; 2001].

With the advanced developments in sensor technology instrument correction has become almost unnecessary for digital recordings. Moreover some researchers proposed using low-pass filtering instead of instrument correction to remove the high-frequency noise since the latter may excessively increase the high-frequency noise due to improper numerical differentiation schemes. Noise models were established to determine the signal/(signal+noise) ratios to decide on the high- and low-pass filter corner frequencies to remove the signals that are contaminated by low- and high-frequency noise [Lee and Trifunac, 1990, Skarlatoudis *et al*, 2003]. Alternatively, some filtering schemes [Boore and Bommer, 2005; Akkar and Bommer, 2006] make use of the low-frequency behavior of the Fourier acceleration spectrum to choose the appropriate high-pass filter corner frequency that ensures consistent decay of spectral amplitudes in the low-frequency range with a theoretical source spectrum [e.g., Brune, 1970; 1971; Atkinson and Silva, 2000]. Recently, Douglas and Boore [2011] proposed a procedure to determine a proper low-pass filter corner frequency by making observations on the high-frequency behavior of Fourier acceleration spectrum. Discussions on different filtering types have concluded that acausal (zero-phase) filters should be favoured over causal filters because they result in more stable peak ground-motion values and spectral ordinates due to the minimum interference of filter corner frequencies with the processed data [Boore and Akkar, 2003; Boore, 2005; Boore and Bommer, 2005].

The major complication in time-domain acausal filtering is the requirement of leading and trailing zero pads at the beginning and end of the recording to accommodate the filter transients. The length of zero pads depends on the filtering frequency and can increase the size of the processed time series significantly for lower filter corner frequencies. The use of such long acceleration time series can be impractical for the response history analysis of large structural systems due to computer run-time as well as the internal memory problems experienced by some of the structural analysis programs. Thus, some end users, incautiously, remove these padded sections that essentially eliminate the acausal filtering effects and results in an inconsistency in the processed data [Boore, 2005; Boore and Bommer, 2005]. In order to prevent such inconsistencies, some agencies (e.g., ITACA [3] and PEER NGA [4]) apply a type of post-processing procedure to the acausally filtered data after removing the zero pads and disseminate the ground acceleration, velocity and displacement time series as well as the response spectra and peak ground motion values of the post-processed data [see details in Boore *et al*, 2012].

As it can be appreciated from the above discussions, the number of data processing schemes is large and the major challenges are the influence of different processing schemes on the ground-motion parameters and the determination of the usable spectral period range where the influence of processing is minimal. The usable period band should be as wide as possible to address a large range of engineering applications as noted in the previous paragraph. For this particular issue, Abrahamson and Silva [1997] used spectral ordinates if the spectral period is less than 0.8 times the high-pass corner period and greater than 1.25 times the low-pass corner period. As a common decision, NGA model developers continued using these fractions while developing their predictive equations. This approach assumes that high- and low-pass corner frequencies symmetrically affect the response spectral ordinates. Akkar and Bommer [2006] also showed that the spectral response is influenced by the chosen high-pass filter cut-off at spectral periods beyond some proportion of the high-pass filter value. Contrary to Abrahamson and Silva [1997] or NGA model developers, who implemented a constant fraction of high-pass filter cut-off period, the proposed proportions of Akkar and Bommer [2006] range between 0.65 – 0.95 depending on the instrument type (i.e., analogue vs. digital) and recording site characteristics. . Paolucci *et al* [2008] indicated that the usable period range of high quality digital recordings extend to 10s, if a high-pass filter value of 20s (i.e., 0.05 Hz) is applied regardless of their size, location with respect to source and site class. (Note that for a high-pass filter cut-off value of 20s,

Akkar and Bommer [2006] recommend using the spectral ordinates up to 19s for digital recordings from soft sites). Using a set of different noise models, Akkar and Boore [2009] concluded that high-quality digital recordings could be used for spectral periods up to 10-20s after the application of the simplest baseline correction procedure (i.e., removing the mean of the pre-event segment from the entire accelerogram). Douglas and Boore [2011] demonstrated that short-period response spectral ordinates are less sensitive to the low-pass filter cut-off, because short-period response spectral ordinates are controlled by lower frequency motion since the higher frequency ground-motion components attenuate at most sites except those located on very hard rock. This observation disagrees with the use of symmetrical influence of high- and low-pass filter corners on the spectral ordinates. This conclusion led Akkar *et al* [2011] to suggest extending the short-period limit of pan-European strong-motion database to at least 0.02s. The NGA ground-model models use  $T=0.01s$  as the shortest period for the calculation of spectral ordinates.

### 9.3 Interpolation

Discussions in the above paragraphs and the previous section address the importance of high-quality and reliable ground-motion metadata for the development of new GMPEs. This is also important in testing the current ground-motion models for use in hazard analysis in different seismotectonic regions. Well-constrained strong-motion datasets constitute the primary basis for the reliable evaluation of candidate GMPEs.

As noted above, recent research has shown that the usable spectral period range of high-quality recordings can extend from 0.01-0.02s to 15-20s, which should be the target period band for future GMPEs. Most of the current GMPEs, except for those developed in the NGA project, lack such a wide period band due to various reasons. The NGA models are able to estimate spectral ordinates between 0.01s and 10s although the number of recordings used in the regression analysis drops-off drastically after  $T = 5s$ . This limitation can require interpolation of the current models for some intermediate periods provided that both ends of the interpolation interval are fixed, if so required for a particular application (e.g., testing of GMPEs at previously defined periods specific to the needs of the project or for PSHA studies). When interpolation is required, it can be done either directly on the predicted spectral ordinates or on the regression coefficients. There is readily available software that implements the former approach for the NGA ground-motion models (NGA\_GM\_TMR; Next Generation Attenuation Ground Motions for Specified Period, Magnitude and Distance [5]). The second alternative is more flexible and general because it offers a wider range of applicability of the interpolated GMPEs. Nevertheless caution should be exercised in this alternative if the functional form of the interpolated model is complex and contains a large number of coefficients. A recent study by Bommer *et al* [2012] showed that interpolation at the short-period end of the spectral ordinates can be done successfully by assuming that the spectral ordinate at  $T = 0.01s$  can be represented by PGA except for very hard rock conditions (e.g., Eastern North America) for which interpolation can result in non-conservative values. Bommer *et al* [2012] perform the coefficient interpolations using cubic splines either in the linear or logarithmic domain depending on the original period spacing of the subject ground-motion model. The suggested approach produces reasonable results for GMPEs from active regions even if the original shortest response period of the model is  $T = 0.1s$ . For very hard rock site conditions this approach will not yield reliable results unless the equation includes coefficients for the spectral ordinates down to at least 0.04s or 0.03s at least. Bommer *et al* [2012] conclude that the key issue for the success of interpolation is that the fixed spectral ordinate at the far-end of the short-period range should be smaller than the response period at

which the peak of the response spectrum occurs. The extrapolation of GMPEs is strongly discouraged in both short- and long-period ranges.

#### 9.4 Horizontal Component Definitions

The current ground-motion models use either the as-recorded geometric mean or GMROTI50 [Boore *et al*, 2006] as the definition of the horizontal component. Both definitions consider the directional uncertainty in the horizontal ground motions. Definition of GMROTI50 requires equal length horizontal components for its calculation. These horizontal component definitions can be considered as ideal for estimating horizontal ground motion and there are empirical equations to relate these two horizontal component definitions [e.g., Beyer and Bommer, 2006; Watson-Lamprey and Boore, 2007]. In combination with these horizontal component definitions, consideration of fault-normal and fault-parallel horizontal components is important for models that address the near-fault effects on ground motions. All of the horizontal components designated with a GM term can be used for this current GEM Global Ground Motion Component-PEER project, except the GMRotD100 (the maximum value of ground motion at any azimuth). Please monitor the findings of the NGA-West2 [4] Directivity and Directionality Working Group chaired by Paul Spudich and Jack Baker).

#### 9.5 Other Ground Motion Parameters used in GMPEs

The predictive models should also consider other ground-motion parameters for a complete description of ground motion. Such parameters include equivalent number of cycles, strong-motion duration, spectral ratios at different damping values, horizontal-to-vertical spectral ratios, Arias intensity, cumulative absolute velocity, etc. The third and fourth topics are being address in the PEER NGA-West2 [4] project. These parameters can be of particular use either as supplementary to the conventional amplitude-based ground-motion parameters or for responding to the needs of more advanced design/risk assessment projects. For example, estimates of the equivalent number of cycles [e.g., Seed and Idriss, 1971; Liu *et al*, 2001; Stafford and Bommer, 2009] are useful to account for the assessment of liquefaction and earthquake-induced landslides. Scaling (or correction) factors for response spectral ordinates of different damping ratios [e.g., Atkinson and Pierre, 2004; Lin *et al*, 2005; Bommer and Mendis, 2005; Cameron and Green, 2007; Stafford *et al*, 2008] are of particular use in displacement-based design/assessment procedures as well as for the design of base-isolation systems. Strong-motion duration, depending on the structural type, structural detailing and the construction material, can be a measure of structural damage. It is also an important parameter to determine the possibility of liquefaction as it strongly influences the build-up of pore pressure during ground shaking. Moreover, when the strong-motion duration is used together with Arias intensity, this can establish a useful background for the stochastic simulation of ground motions, which can be used for specific engineering projects [e.g., Pousse *et al*, 2006].

Arias intensity, as a standalone parameter, has been used as an index of damage for many geotechnical and structural engineering problems. Because of this Travarasrou *et al* [2003] developed a recent predictive model for this parameter as a function of magnitude, distance, site class and style-of-faulting. There are also older and more recent predictive models for Arias intensity in the literature [e.g., Campbell and Duke, 1974; Wilson and Keefer, 1985; Kayen and Mitchel, 1997; Paciello *et al*, 2000]. Cumulative absolute velocity (CAV) has been shown to be a very good predictor of damage-related phenomena, such as liquefaction and structural damage, as noted by Campbell and Bozorgnia [2011a]. Furthermore, Campbell and Bozorgnia

[2010, 2012] show that CAV has a sigma that is 50% smaller than Arias intensity, important for deterministic as well as PSHA studies. Because of this, Campbell and Bozorgnia [2010, 2011b] developed predictive models for both CAV as well as a version of CAV that excludes non-damaging ground motions from its computation. Since vertical ground motions are also important for the design of many structural systems including the critical facilities including nuclear power plants, information on vertical spectral ordinates is essential for engineers [Bozorgnia and Campbell, 2004a]. There are many predictive models that estimate vertical spectral ordinates [see Bozorgnia and Campbell, 2004b; and Bommer *et al* 2011 for an extensive review of such GMPEs] but the recent trend among model developers is to derive horizontal-to-vertical spectral ratio GMPEs [e.g., Gülerce and Abrahamson, 2011; Bommer *et al*, 2011; Bozorgnia and Campbell, 2004b] in order to provide vertical spectra consistent with the horizontal spectral ordinates derived from a seismic hazard analysis. This is a topic being addressed in the PEER NGA-West2 [4] project. Derivation of consistent vertical spectra from horizontal spectral ordinates requires additional information on the correlation of spectral ordinates (i.e., orthogonal ground-motion components; another important ground-motion parameter to be estimated by the predictive models). A considerable amount of work has already been completed on the correlation models between spectral ordinates at different vibration periods and for orthogonal ground-motion components by Baker and Cornell [2004; 2005; 2006a; 2006b] that can be used efficiently for vector-valued probabilistic seismic hazard analysis [Bazzurro and Cornell, 2002] or in calculating a Conditional Mean Spectrum [Baker, 2011] to provide more realistic information about the spectral content of the ground motions occurring at a site; thus increasing the precision of structural response analysis. In addition to these ground-motion parameters, future predictive models will extensively involve the estimation of inelastic spectral ordinates and inelastic-to-elastic spectral ordinate ratios in the near future to mimic the actual ground-motion demand on different structural systems responding beyond their elastic limits. Preliminary efforts on these ground-motion intensity measures have already started to provide some valuable information that can be used significantly in future seismic hazard analysis [e.g., Tothong and Cornell, 2006; Bozorgnia and Campbell, 2010; Ruiz-Garcia and Miranda, 2007].





## 10 Consideration of Simulation-based GMPEs

The earthquake source involves a complex rupture process on a fault, seismic waves arrive at the site by propagation through a complex waveguide, and complex local geology can have an important influence on the recorded ground motions. Strong-motion simulation methods have the advantage of allowing the incorporation of information about earthquake source, seismic wave propagation, and local site characteristics that are specific to the region and to a specific site location. These characteristics may include rupture directivity effects, hanging wall/foot wall effects, Moho bounce effects, basin effects, and site effects. The simulation methods have the potential to generate accurate representations of the ground motions when strong motion recordings are unavailable. This is contingent upon the use of simulation methods that have the capability to accurately reproduce the characteristics of recorded ground motions in cases where the earthquake source and seismic velocity structure (and hence wave propagation characteristics) are well known, and upon the availability of reliable information about earthquake source and crustal structure characteristics in the site region. When the simulated ground motions are used in the development of GMPEs, however, these source and site-specific effects might be averaged out.

Modern seismic hazard analysis for regions of sparse data (e.g., stable continental regions or active crustal regions with limited number of strong-motion recordings) generally requires GMPEs that are based on ground-motion simulations because the available observational data in such regions are insufficient to properly constrain the ground-motion variation<sup>4</sup>. Even in tectonically active regions, the ground motions that dominate seismic hazards at return periods used in seismic design are often for large earthquake magnitudes and close distances; there are few records in the strong-motion databases at such magnitudes and distances. Synthetic accelerograms can also supplement the strong-motion database where the data distribution is poorly constrained in terms of independent estimator parameters such as magnitude, distance and style-of-faulting etc. Stochastic (either point- or finite source) and broadband simulation methods can be used to develop GMPEs for determining the deterministic and probabilistic estimates of design ground motion. In addition to recent simulation-based GMPEs, the hybrid empirical method has become popular. This approach estimates ground motions in regions of limited data (target regions) by calibrating reliable GMPEs from regions of abundant data (host regions). This chapter discusses the use of simulation procedures for developing GMPEs; these GMPEs, in turn, can be used in seismic hazard assessments for earthquake-prone regions lacking sufficient empirical data. Douglas and Aochi [2008] critically review more than twenty methods for ground-motion prediction that have been proposed in the literature.

---

<sup>4</sup> Campbell [2003] indicated that intensity-based relationships are alternatives to simulation-based GMPEs for regions of sparse data for predicting quantitative ground-motion parameters from qualitative measures of ground shaking such as Modified Mercalli Intensity (MMI). Intensity-based methods are applied by estimating seismic intensity from an attenuation relationship then estimating the ground-motion parameter using a relationship between ground-motion and intensity [Wald et al., 1999]. Intensity-based relationships are outside the scope of this chapter.

## 10.1 Point Source Stochastic Simulation Methods

Stochastic simulations of ground motions assume that the energy represented by a specific Fourier amplitude spectrum is distributed randomly over a duration that depends on source-size and propagation distance. The assumption of randomness is most applicable for high-frequency ground motions of engineering interest. Stochastic simulation procedures have their roots in the collaborative works of Hanks and McGuire who treated the source as a point [Hanks, 1979; McGuire and Hanks, 1980; Hanks and McGuire, 1981]. Boore [1983, 2003] generalized the point-source stochastic simulation procedure that originated in the above cited references for complex source models for generating time series as well as other ground motion intensity measures such as response spectrum. One of the well-known point-source stochastic simulation programs, SMSIM, was also developed by Boore [2005; the updated version of the software can be found at [www.daveboore.com](http://www.daveboore.com)].

The acceleration time series generated by stochastic point-source models feature both deterministic and random aspects of ground-motion shaking. The deterministic aspects are described by the magnitude- and distance-dependent average Fourier spectrum whereas modeling the motions as noise mimics the random nature of the ground motions. The point-source assumption is reasonable when the source-to-site distance is much larger than the source dimensions [Boore and Atkinson, 1987; Atkinson and Boore, 1995; 1997; Atkinson and Silva, 1997; 2000]. The theoretical total point – source spectrum,  $Acc(M_0, R, f)$ , is calculated by the following equation:

$$Acc(M_0, R, f) = Source(M_0, f) Path(R, f) Site(f) \quad (10.1)$$

where  $Source(M_0, f)$  is the source spectrum at unit distance from the source;  $Path(R, f)$  is the path effect that includes the effects of both geometrical spreading and an elastic attenuation;  $Site(f)$  is the site response operator that includes both site-dependent modification of spectral amplitudes and high-frequency attenuation that is mainly addressed by  $\kappa$  [Hanks, 1982; Anderson and Hough, 1984]. The site-dependent modification includes both the amplification of the waves from the source as well as the near-surface effects. Most of the seismological parameters that describe the variation of each major component in Eq. (10.1) are region specific and should be derived from the high-quality seismological data that are available in the region. The reader is referred to Boore [2003] for the details of stochastic point-source simulation methods.

## 10.2 Extended Source Simulation Methods

### 10.2.1 Stochastic Finite Source Simulation Methods

The simplest extended-source simulation method is stochastic finite-source model and it accounts for the effects of faulting geometry, distributed rupture and rupture inhomogeneity that are not considered in the stochastic point-source model. Finite fault effects were addressed by Hartzell [1978] who proposed dividing the fault surface of an earthquake into a grid of subsurfaces, each of which could be treated as a point-source. Beresnev and Atkinson [1998a] applied  $\omega^2$  stochastic point-sources to each of the subsurface activities to adapt the stochastic approach to a finite-source model. Beresnev and Atkinson [1998b] developed FINSIM, a computer program, which implements this approach. Later Motazedian [2002] and Motazedian and Atkinson [2005] modified FINSIM as EXSIM to minimize the dependence of the simulation results of the former software on subsurface size. In EXSIM each subsurface is activated once with an appropriate delay time of  $\Delta t_i$ . Boore [2009] proposed a modification to the original version of EXSIM that results in a better comparison of the point-source and extended-source simulations for moderate-to-small magnitudes at large distances.

The stochastic simulations resulting from point-source and extended-source simulations can be different due to the complex trade-offs between the factors. The geometry and distance definitions are not the same in these approaches. The geometry is a point and the most efficient distance measure is hypocentral distance in stochastic point-source simulations when they are compared with the estimated ground motions from GMPEs. This point is also observed in different studies [e.g., Scherbaum *et al*, 2006] but Akkar and Yenier [2009] indicated that the performance of  $R_{hyp}$  as the distance measure in stochastic point-source simulations depends on the soil properties of the site and magnitude range of the earthquake scenario. In stochastic finite-source modeling, the geometry is a plane and the most representative distance definition is  $R_{rup}$  that can consider the rupture process at each subsource. Thus, the distance measures in point-source and finite-source stochastic simulation procedures are different and are only equivalent for moderate events at large distances. Therefore, when comparing finite-source and point-source stochastic simulations one should expect differences in predicted ground motions that are attributable to different effective distances at which the source is located relative to the observation point. Boore [2009] proposed an alternative distance definition: effective distance ( $R_{eff}$ ) for improved consistency between the point- and finite-source stochastic simulations.

The origin of source and distance-dependent duration terms can also make a difference between the finite-fault and point-source stochastic simulations. In point-source simulations the duration is specified as the source duration that is based on event corner frequency plus a distance-dependent duration term. In finite-source simulations the total time of radiation from the source is controlled largely by the time required for rupture propagation along the length of the fault as each subsource ruptures in turn and is then delayed accordingly to its arrival at a specific location. Additionally, in finite source stochastic models each subsource has a distance-dependent duration term that is added at the observation point. Differences in duration between stochastic point- and finite-source simulations can result in different response spectral amplitudes.

In general the stochastic point-source and finite-fault simulation methods treat the source effects in a simple way and they do not include the possible effects of, for example, rupture mechanism and depth. Varying the stress parameter in stochastic simulation techniques can be used to adjust for these effects. The point-source approach has the advantage of simplicity and can be manipulated to mimic the salient finite-fault effects by an appropriate modification of the distance measure [Boore, 2009]. The finite-fault approach is more flexible in modeling extended faults and exploring their effects on ground motions. Stochastic simulation methods should be used for generic or region-specific applications for which the average motions from a suite of earthquakes are desired (as in the case of developing simulation-based GMPEs). Their use for path-specific and local applications depends on the accuracy of the input parameters of the model [Frankel, 2009].

Predictive models that are derived from stochastic simulation methods rely on the availability of local seismic data from small events to properly address source, path and site effects that include the regional crustal model, type of spectrum, stress parameter, geometric attenuation, source and path duration, local site diminution and soil profile etc. These parameters can be described by probability distributions to account for the inherent aleatory variability in ground motions (e.g., Atkinson and Boore, 2006). Although the description of source, path and site effects from local seismic data has been done in a reliable manner for many seismic prone regions around the world (e.g., Eastern North America, Peninsular India and a few European countries etc.), it is difficult to identify reliable studies for many other seismic regions. In such cases stochastic simulations have to make particular assumptions in adopting source, path and site functions derived in other studies. Such a situation may result in poor simulation-based GMPES that may fail to represent the actual ground motion variation for the region under study. The GMPEs that are developed from stochastic simulations may also fail to represent the epistemic uncertainty because they are mainly based on a single

methodology [Campbell, 2003a]. (An exception is the ground-motion model derived by Silva *et al* [2002] that captures the epistemic variability by performing stochastic simulations by varying the stochastic model). A proper estimation of epistemic uncertainty is important for defining the design ground motion and should be included in seismic hazard assessment.

### 10.2.2 Hybrid Methods to Simulate Broadband Ground Motions

The stochastic methods previously discussed are most appropriate for high-frequency ground motions. While these motions are applicable for most frequencies of engineering interest, there are a number of low-frequency structures (e.g., long-bridges, tall buildings, storage tanks) for which the deterministic modeling of ground motion would be more appropriate. These deterministic methods model the actual rupture process and seismic wave propagation on a finite fault with a physically reasonable source description that is usually kinematics but can also be dynamic. The stochastic and deterministic simulations are now being combined as a hybrid method that simulates ground motions over a wide frequency range. These methods are commonly referred to as broadband simulation methods. They are hybrid in the sense that they combine deterministic simulations at low frequencies and stochastic simulations at high frequencies.

The hybrid method uses the elastodynamic representation theorem, which states that the ground motion  $U(t)$  can be calculated from the convolution of the slip time function  $D(t)$  on the fault with the Green's function  $G(t)$  for the appropriate distance and depth, integrated over the fault rupture surface:

$$U(t) = \sum D(t) * G(t) \quad (10.2)$$

The earthquake source is represented as a shear dislocation on an extended fault plane. The radiation pattern of the source, and its tendency to become subdued at periods shorter than about 0.5 sec, are represented.

In the Empirical Green's Function method [Hartzell, 1978; Irikura and Kamae, 1986; Kamae *et al*, 1998], the Green's function is empirically embodied in the recordings of small earthquakes that are used in a summation process to model the rupture of a larger earthquake. This method is only viable if ground motion recordings that span the required ranges of distances and depths in an appropriate crustal model are available. Otherwise, it is necessary to calculate the Green's functions for the seismic velocity structure, which contains the fault and the site.

When Green's functions are calculated, a hybrid procedure is usually used in which broadband ground motions are obtained by combining long-period synthetic seismograms with partly stochastic short-period ground motion simulations<sup>5</sup>. The long-period synthetic seismograms are derived from deterministic methods for reproducing the coherent phases on actual strong-motion records including body waves (such as the pulses that are caused by forward rupture directivity), and surface waves. The deterministic approach also represents the realistic delay and phasing of long-period surface waves relative to the S-waves. The short-period simulations are usually developed from point-source stochastic simulation methods. The long-period

---

<sup>5</sup> There are alternative broadband simulation methods such as the one proposed in Pacor *et al*. [2005], the so-called Deterministic-Stochastic Method – DSM, that modifies the model of Boore [1983, 2003] by introducing a deterministic envelope by solving a simplified formulation of the representation theorem [Aki and Richards, 1980] and deterministically deriving the reference omega-squared spectrum. Synthetics modeled by DSM are sensitive to the direction of rupture over the fault with respect to site and rupture starting point.

synthetic seismograms and short-period simulations are summed over the finite-fault to simulate the actual accelerogram for a given scenario.

Broadband simulations as described above have been the topic of research in various studies [e.g., Irikura and Miyake, 2001; 2011; Graves and Pitarka; 2004, 2010 Hartzell and Heaton, 1995; Hartzell *et al*, 1999]. At frequencies below 1 Hz, the methodology is deterministic and contains a theoretically rigorous representation of fault rupture and wave propagation effects, which can reproduce recorded ground motion waveforms and amplitudes. The Green's functions are often calculated for a 1D crustal structure, but it is also possible to calculate them for a 3D structure [Graves and Pitarka, 2004; 2011], in which case separate Green's functions are required for each combination of fault element and recording site. At frequencies above 1 Hz, the broadband methodology uses a stochastic representation of source radiation, which is combined with a simplified theoretical representation of wave propagation and scattering effects.

The use of different simulation approaches for the different frequency bands is in accord with the seismological observation that source radiation and wave propagation effects tend to become stochastic at frequencies of about 1 Hz and higher. Complexities in the rupture process and scattering by random homogeneities in the crust between the source and receiver cause incoherence in the summation of waveforms produced by different parts of the rupture process. The transition frequency between coherent and incoherent summation may vary with magnitude [Frankel, 2009].

The major aim of broadband simulations is to represent the actual ground motions as realistically as possible, so several important intermediate steps are involved. For deterministic (long-period) synthetic seismograms (a) Green's functions are calculated for a range of distance and source depths, (b) the fault plane (whose size is consistent with the scenario magnitude) is divided into set of subfaults, (c) the distribution of slip and/or stress drop on the fault is specified (with slip sometimes being described by a fractal distribution as a function of wave number), (d) the long-period Green's functions are convolved with a source time function for each subfault, and (e) the rupture arrival time for each point on the fault plane is defined, in the simplest case assuming constant rupture velocity.

The stochastic (short-period) synthetics for each subfault are multiplied by a stress drop factor derived either from a fractal distribution of stress drop or from the fractal slip used for the long-period synthetics. This step requires a proper description of stress drop. The stochastic synthetics also require the other seismological parameters (e.g., anelastic and geometric spreading and,  $\kappa$ ) for reliable generation of short-period waveforms. After the point source stochastic synthetics are summed over the fault plane they are convolved with a source time function that ensures that the Fourier acceleration spectrum is flat for frequencies less than the corner frequency used for subevents and frequencies greater than the transition frequency with the long-period synthetics.

The large number of seismological parameters that are necessary for broadband simulation methods place significant demands for their implementation for the development of simulation-based GMPEs. Nonetheless there are various validation studies that compare broadband synthetics with actual earthquake recordings or ground-motion estimations of empirical GMPEs [e.g., Graves and Pitarka, 2004; 2010; Frankel, 2009; Ameri *et al*, 2009]. Moreover, a Platform for Broadband Strong Motion Simulation has recently been developed by the Southern California Earthquake Center. This platform can be accessed at [http://scec.usc.edu/scecpedia/Broadband\\_Platform](http://scec.usc.edu/scecpedia/Broadband_Platform). These developments support the use of broadband simulation technique for strong-motion applications. For example, the recent simulation-based predictive model of Somerville *et al* [2009] used broadband simulations following the hybrid method in Graves and Pitarka [2004; 2010] based on the finite-fault rupture models of large Australian earthquakes through the

inversion of teleseismic waves, geodetic and surface faulting data. The deterministic and stochastic synthetics are combined at 1 Hz using matched filters. Green's functions are calculated from validated crustal structure models of Australia. The fault models are used to derive earthquake source models for their use in strong-motion simulations by including constraints for the scaling relationship between seismic moment and rupture area. Thus, this simulation-based ground-motion model can account for the known source and crustal structure properties of Australia.

### 10.3 Hybrid Empirical Methods

The hybrid empirical approach was proposed by Campbell [2003a, 2003b] and uses theoretically-based adjustment factors to estimate ground motions in a region where the strong-motion records are few. Using stochastic point-source simulations the method develops adjustment factors from the ratios of theoretical ground motions produced for regions of limited strong-motion records (target region) and regions where good empirical GMPEs exist due to abundant strong-motion data (host region). (The stochastic point-source simulation approach is the most commonly-used methodology for generating theoretical ground motions but any other simulation technique is equally applicable for the implementation of the hybrid empirical method). The major aim of the method is to modify the GMPEs of the host region for the target region through theoretical adjustment factors on the basis of seismotectonic differences (source, path and site effects) between these regions.

The foundation of the hybrid empirical model was developed by Campbell [1981, 1982, 1987, 2000a]. Several researchers made use of the preliminary versions of the hybrid empirical model [e.g., Abrahamson and Becker, 1997; Stepp *et al*, 2001; Savy *et al*, 1999; Tavakoli and Pezeshk, 2005; Pezeshk *et al*, 2011] but its formal mathematical framework was published in Abrahamson and Becker [1997] and Campbell [2001a; 2001b]. The method has been used by several authors to predict strong-ground motion in Eastern North America [Atkinson, 2001; Abrahamson and Silva, 2001; Campbell, 2003a; 2003b].

In the application of the hybrid empirical model the host region should have one or more empirical GMPEs to estimate the ground-motion parameters of interest. Both regions should have one or more seismological models that can be used to characterize the regional source spectra, crustal velocity structure, wave propagation characteristics and local site characteristics. An estimate of the ground motion in the host region is computed using the stochastic point-source method and the stochastic model for the host region, and a similar estimate is made for the target region using the stochastic model of the target region including the weighting for the different choices of parameters. The ratio of these two estimates is used to adjust the ground motion of the host region derived from empirical GMPEs.

One of the strengths of the hybrid empirical model is its ability of providing estimates of both aleatory and epistemic uncertainty in the estimated ground-motion parameter. This advantage is particularly important in PSHA. The epistemic uncertainty in the hybrid empirical model is accounted for by different seismological models used in stochastic simulations. For example stress parameter and crustal attenuation are typical examples of parameters that could be included in addressing the epistemic uncertainty. The epistemic uncertainty in the host region is generally disregarded as the seismological models in the host region are usually calibrated from strong-motion records. The epistemic uncertainty in the host region is considered by assuming distributions for each seismological parameter in the stochastic point-source simulations. The aleatory variability in hybrid empirical model is attributed to the spread around the theoretical ground motions that originates from the GMPEs used in the host region and the additional aleatory variability in the host GMPEs that results from excluding one or more empirically modeled stochastic parameters in its



estimation (e.g., faulting mechanism that is not used in deriving the empirical estimates of ground motion that are obtained from the host GMPEs). The use of multiple GMPEs will also be an additional input to address the epistemic uncertainty.

The hybrid empirical method as presented above is analogously used by Atkinson [2008] to scale a base (host) ground-motion predictive model by using the empirical earthquake data in the target region. (This method is referred to as the Referenced Empirical method, see Atkinson and Boore [2011] for a modification of the Atkinson [2008] implementation of this method]. This approach fits distance- and magnitude-based equations on the residuals computed from the base model and observed empirical data in target region to adjust the estimates of host GMPE according to the seismological and tectonic features of target region.

Douglas *et al* [2006] implemented the composite model technique [Scherbaum *et al*, 2005] to develop simulation-based GMPEs for southern Spain and southern Norway. The method is also inspired by the hybrid empirical technique and aims at transporting one or more empirical ground-motion relations from a host region to a target region. This process is done in a comprehensive way by using the ground-motion component of logic trees. Each candidate ground-motion relation from a host region is considered as a branch of the logic tree with its own weights and epistemic uncertainty. Thus, a set of equations is derived (one for each host equation) with an adjustment by the host-to-target relationships.

The composite model technique generates a ground-motion dataset for the logic trees corresponding to scenarios defined by different combinations. Each combination consists of a particular ground-motion model that is subjected to a prior unification in terms of magnitude, distance, style-of-faulting distribution and horizontal component combination. (The significance of these conversions is described in detail in the previous chapters of this report). This conversion is performed using a Monte Carlo simulation that retains the scatter induced by undertaking these conversions. In this way the uncertainties are added or propagated by accounting for the influence of uncertainties in each of the conversions. These estimated ground motions are then scaled using the ratios of estimated host-to-target conversion factors derived using the point-source stochastic simulations. The scaled ground motions are used in regression analysis to develop a set of ground-motion equations for the target region.

The uncertainties in host host-to-target relations are handled in a similar way thorough logic trees (i.e., different stochastic models due to variations and poor information on source spectrum, stress drop, geometrical spreading, anelastic attenuation  $Q(f)$ , site conditions as a function of shear-wave velocity profiles and near-source attenuation,  $\kappa$ ) and, for example, magnitude and distance conversions. The stochastic models for each of the host GMPEs are obtained by a genetic algorithm search presented in Scherbaum *et al* [2005]. Essentially, in this technique, the ground motion sections of a complete logic tree for probabilistic hazard are treated as a single composite model, which mimics the complete state-of-knowledge-and-belief of a particular analyst on ground motion in a particular target region. The application of logic tree results in a transparent description of the spread of the composite model expressed by the distribution of quantiles that captures all the epistemic uncertainties. In fact this is the major difference between the composite and hybrid empirical models. The resulting ground-motion models can be directly implemented in PSHA associated with their properly assigned weights and, therefore, the epistemic uncertainty is not combined with the aleatory uncertainty [Budnitz *et al*, 1997] when PSHA is performed.

## 10.4 Efficiency of Simulation Methods for Simulation-based GMPEs and PSHA

The simulation methods described in this chapter have been used for developing GMPEs for regions where strong-motion records are limited. All of these methods depend on a detailed parameterization where the

assessment of simulated ground motions and related uncertainties may be difficult for regions that are poorly covered by seismological networks and studies. The ideal target regions are therefore those with a rate of seismicity such that the path and site properties can be determined from small magnitude earthquakes. In PSHA implementation for regions that lack strong-motion data, GMPEs derived from point-source and extended-source stochastic simulations (that properly address epistemic uncertainty) are appealing as these methods are easy to apply. The stochastic methods can also be used efficiently in hybrid empirical and composite techniques, which can also be considered for PSHA studies of regions lacking GMPEs due to sparse strong-motion data. The consistent use of stochastic methods in PSHA depends on their suitability for the region under consideration. Their validity can be checked with regional empirical data, given that such data exists. Provided that adequate knowledge of the seismological parameters is available, the hybrid simulation techniques can be used in site-specific PSHA studies. The hybrid methods can also account for the epistemic uncertainty and are capable of addressing the propagation of uncertainties on the simulated ground motion parameters.



## References

- Abrahamson N.A. [2000] "Effects of rupture directivity on probabilistic seismic hazard analysis," *Sixth International Conference on Seismic Zonation*, Earthquake Engineering Research Inst., Oakland, CA.
- Abrahamson N.A., Youngs R.R. [1992] "A stable algorithm for regression analysis using the random effects model," *Bulletin of the Seismological Society of America*, Vol. 88, pp. 505–510.
- Abrahamson N.A., Becker A.M. [1997] "Ground motion characterization at Yucca Mountain, Nevada," Report submitted to the U.S. Geological Survey that fulfils Level4 Milestone SPG28EM4 WBS No. 1.2.3.2.8.3.6.
- Abrahamson N.A., Silva W.J. [1997] "Empirical response spectral attenuation relations for shallow crustal earthquakes," *Seismological Research Letters*, Vol. 68, pp. 94–127.
- Abrahamson N.A., Silva W.J. [2001] "Empirical attenuation relations for central and eastern U.S. hard and soft rock and deep soil site conditions," *Seismological Research Letters*, Vol. 72, pp. 282.
- Abrahamson N.A., Silva W.J. [2007] "Abrahamson and Silva NGA ground motion relations for the geometric mean horizontal component of peak and spectral ground motion parameters," Preliminary PEER Report dated October 19, 2007, Pacific Earthquake Engineering Research Center, Berkeley, CA, 380 pgs.
- Abrahamson N.A., Silva W.J. [2008] "Summary of the Abrahamson and Silva NGA ground motion relations," *Earthquake Spectra*, Vol. 24, pp. 67–97.
- Abrahamson N.A., Gregor N., Addo K [2012] "BCHydro ground motion prediction equations for subduction earthquakes," *Earthquake Spectra* (submitted).
- Akkar S., Bommer J.J. [2006] "Influence of long-period filter cut-off on elastic spectral displacements," *Earthquake Engineering and Structural Dynamics*, Vol. 35, pp. 1145–1165.
- Akkar S., Boore D.M. [2009] "On baseline corrections and uncertainty in response spectra for baseline variations commonly encountered in digital accelerograph records," *Bulletin of the Seismological Society of America*, Vol. 99, No. 3, pp. 1671–1690.
- Akkar S., Yenier E. [2009] "Assessment of point source stochastic simulations using recently derived ground-motion prediction equations," *Bulletin of the Seismological Society of America*, Vol. 99, pp. 3172–3191.
- Akkar S., Çagnan Z., Yenier E., Erdogan Ö., Sandıkkaya A. Güllan P. [2010] "The recently compiled Turkish strong motion database: preliminary investigation for seismological parameters," *Journal of Seismology*, No. 14, pp. 457–479.
- Akkar S., Kale O., Yenier Y., Bommer J.J. [2011] "The high-frequency limit of usable response spectral ordinates from filtered analogue and digital strong-motion accelerograms," *Earthquake Engineering and Structural Dynamics*, Vol. 40, pp. 1387–1401.
- Aki K., Richards P.G. [1980] *Quantitative Seismology: Theory and Methods*, Vol. 1 and 2, W.H. Freeman, San Francisco, CA, 932 pgs.

- Ambraseys N.N., Smit P., Douglas J., Margaris B., Sigbjornsson R., Olafsson S., Suhadolc P., Costa G. [2004] "Internet site for European strong-motion data," *Bollettino di Geofisica Teorica ed Applicata*, Vol. 45 no. 3, pp. 113–129.
- Ameri G., Gallovič F., Pacor F., Emolo A. [2009] "Uncertainties in strong ground-motion prediction with finite-fault synthetic seismograms: An application to the 1984 M 5.7 Gubbio, central Italy, earthquake," *Bulletin of the Seismological Society of America*, Vol. 99, pp. 647–663.
- Atkinson G.M. [2001] "An alternative to stochastic ground-motion relations for use in seismic hazard analysis in eastern North America," *Seismological Research Letters*, Vol. 72, pp. 299–306.
- Atkinson G.M. [2006] "Single-station sigma," *Bulletin of the Seismological Society of America*, Vol. 96, No. 2, pp. 446–455.
- Atkinson G.M. [2008] "Ground-motion prediction equations for eastern North America from a referenced empirical approach: Implications for epistemic uncertainty," *Bulletin of the Seismological Society of America*, Vol. 98, pp. 1304–1318.
- Atkinson G.M. [2010] "Ground-motion prediction equations for Hawaii from a referenced empirical approach," *Bulletin of the Seismological Society of America*, Vol. 100, No. 2, pp. 751–761.
- Atkinson G.M., Boore D.M. [1995] "New ground motion relations for eastern North America," *Bulletin of the Seismological Society of America*, Vol. 85, pp. 17–30.
- Atkinson G.M., Boore D.M. [1997] "Stochastic point-source modeling of ground motions in the Cascadia region," *Seismological Research Letters*, Vol. 68, pp. 74–85.
- Atkinson G.M., Silva W.J. [1997] "Empirical source spectra for California earthquakes," *Bulletin of the Seismological Society of America*, Vol. 87, pp. 97–113.
- Atkinson G.M., Silva W.J. [2000] "Stochastic modeling of California ground motions," *Bulletin of the Seismological Society of America*, Vol. 90, pp. 255–274.
- Atkinson G.M., Pierre J.R. [2004] "Ground-motion response spectra in Eastern North America for different critical damping values," *Seismological Research Letters*, Vol. 75, No. 4, pp. 541–545.
- Atkinson G.M., Boore D.M. [2006] "Earthquake ground-motion prediction equations for eastern North America," *Bulletin of the Seismological Society of America*, Vol. 96, pp. 2181–2205.
- Atkinson G.M., Morrison M. [2009] "Regional variability in ground motion amplitudes along the west coast of North America," *Bulletin of the Seismological Society of America*, Vol. 99, pp. 2393–2409.
- Atkinson G.M., Boore D.M. [2011] "Modifications to existing ground-motion prediction equations in light of new data," *Bulletin of the Seismological Society of America*, Vol. 101, pp. 1121–1135.
- Anderson J.G., Hough S.E. [1984] "A model for the shape of the Fourier amplitude spectrum of acceleration at high frequencies," *Bulletin of the Seismological Society of America*, Vol. 74, 1969–1993.
- Babak A., Krawinkler H. [2004] "Behavior of moment-resisting frame structures subjected to near-fault ground motions," *Earthquake Engineering and Structural Dynamics*, Vol. 33, No. 6, pp. 687–706.

- Baker J.W. [2011] "Conditional Mean Spectrum: Tool for ground-motion selection," *Journal of Structural Engineering (ASCE)*. Vol. 137, pp. 322–331.
- Baker J.W., Cornell C.A. [2004] "Choice of a vector of ground motion intensity measures for seismic demand hazard analysis," *Proceedings of the 13th World Conference on Earthquake Engineering*, Vancouver, B.C.
- Baker J.W., Cornell C.A. [2005] "A vector-valued ground motion intensity measure consisting of spectral acceleration and epsilon," *Earthquake Engineering and Structural Dynamics*, Vol. 34, pp. 1193–1217.
- Baker J.W., Cornell C.A. [2006b] "Correlation of response spectral values for multicomponent ground motions," *Bulletin of the Seismological Society of America*, Vol. 96, pp. 215–227.
- Basili, R. *et al*, 2011, SHARE seismotectonic map, in preparation
- Bazzurro, P., Cornell C.A. [2002] "Vector-valued probabilistic seismic hazard analysis," *Proceedings of the 7th U.S. National Conference on Earthquake Engineering*, Boston, Massachusetts.
- Beresnev I., Atkinson G.M. [1998a] "Stochastic finite-fault modelling of ground motions from the 1994 Northridge, California earthquake, part I: Validation on rock sites," *Bulletin of Seismological Society of America*, Vol. 88, pp. 1392–1401.
- Beresnev I., Atkinson G.M. [1998b] "FINSIM—a FORTRAN program for simulating stochastic acceleration time histories from finite faults," *Seismological Research Letters*, Vol. 69, pp. 27–32.
- Beyer K., Bommer J.J. [2006] "Relationships between median values and between aleatory variabilities for different definitions of the horizontal component of motion," *Bulletin of the Seismological Society of America*, Vol. 96, pp. 1512–1522.
- Bindi D., Luzi L., Massa M., Pacor F. [2010] "Horizontal and vertical ground motion prediction equations derived from the Italian accelerometric archive (ITACA)," *Bulletin of Earthquake Engineering*, Vol. 8, pp. 1209–1230.
- Bird P. [2003] "An updated digital model of plate boundaries," *Geochemistry Geophysics Geosystems*, Vol. 4, o. 3, 52 pgs.
- Bommer J.J., Mendis R. [2005] "Scaling of spectral displacement ordinates with damping ratios," *Earthquake Engineering and Structural Dynamics*, Vol. 34, pp. 145–165.
- Bommer J.J., Scherbaum F., Bungum H., Cotton F., Sabetta F., Abrahamson N.A. [2005] "On the use of logic trees for ground-motion prediction equations in seismic-hazard analysis," *Bulletin of the Seismological Society of America*, Vol. 95, pp. 377–389.
- Bommer J.J., Abrahamson N.A. [2006] "Why do modern probabilistic seismic-hazard analyses often lead to increased hazard estimates?" *Bulletin of the Seismological Society of America*, Vol. 96, pp. 1967–1977.
- Bommer J.J., Stafford P.J., Alarcón J.E., Akkar S. [2007] "The influence of magnitude range on empirical ground-motion prediction," *Bulletin of the Seismological Society of America*, Vol. 97, pp. 2152–2170.
- Bommer J.J., Douglas J., Scherbaum F., Cotton F., Bungum H., Fäh D. [2010] "On the selection of ground-motion prediction equations for seismic hazard analysis," *Seismological Research Letters*, Vol. 81, pp. 783–793.

- Bommer J.J., Akkar S., Kale Ö. [2011] "A model for vertical-to-horizontal response spectral ratios for Europe and the Middle East," *Bulletin of the Seismological Society of America*, Vol. 101, pp. 1783–1806.
- Bommer J.J., Akkar S. [2012] "Consistent source-to-site distance metrics in ground-motion prediction equations and seismic source models for PSHA," *Earthquake Spectra*, Vol. 28, pp. 1–15.
- Bommer J.J., Akkar S., Drouet S. [2012] "Extending ground-motion prediction equations for spectral accelerations to higher response frequencies," *Bulletin of the Earthquake Engineering*, Vol. 10, pp. 379–399.
- Bommer J.J., Douglas J., Strasser F. [2003] "Style-of-faulting in ground motion prediction equations," *Bulletin of Earthquake Engineering*, Vol. 1, pp. 171–203.
- Boore D.M. [1983] "Stochastic simulation of high-frequency ground motions based on seismological models of the radiated spectra," *Bulletin of the Seismological Society of America*, Vol. 79, pp. 1865–1894.
- Boore D.M. [2001] "Effect of baseline corrections on displacements and response spectra for several recordings of the 1999 Chi-Chi, Taiwan, earthquake," *Bulletin of the Seismological Society of America*, Vol. 91, pp. 1199–1211.
- Boore D.M. [2003] "Prediction of ground motion using the stochastic method," *Pure and Applied Geophysics*, Vol. 160, pp. 635–676.
- Boore D.M. [2005] "On pads and filters: Processing strong-motion data," *Bulletin of the Seismological Society of America*, Vol. 95, pp. 745–750.
- Boore D.M. [2005] "SMSIM—Fortran programs for simulating ground motions from earthquakes: Version 2.3—A revision of OFR 96-80-A," *USGS Open-File Report 00-509*, revised 15 August 2005, 55 pgs.
- Boore D.M. [2009] "Comparing stochastic point-source and finite-source ground-motion simulations: SMSIM and EXSIM," *Bulletin of the Seismological Society of America*, Vol. 99, pp. 3202–3216.
- Boore D.M. [2010] "Orientation-independent, nongeometric-mean measures of seismic intensity from two horizontal components of motion," *Bulletin of the Seismological Society of America*, Vol. 100, No. 4, pp. 1830–1835.
- Boore D.M., Atkinson G.M. [1987] "Stochastic prediction of ground motion and spectral response parameters at hard-rock sites in eastern North America," *Bulletin of the Seismological Society of America*, Vol. 77, pp. 440–467.
- Boore D.M., Akkar S. [2003] "Effect of causal and acausal filters on elastic and inelastic response spectra," *Earthquake Engineering and Structural Dynamics*, Vol. 32, pp. 1729–1748.
- Boore D.M., Bommer J.J. [2005] "Processing of strong-motion accelerograms: needs, options and consequences," *Soil Dynamics and Earthquake Engineering*, Vol. 25, pp. 93–115.
- Boore D.M., Atkinson G.M. [2007] "Boore-Atkinson NGA ground-motion relations for the geometric mean horizontal component of peak and spectral ground motion parameters," *Report No. PEER 2007/01*, Pacific Earthquake Engineering Research Center, University of California Berkeley, CA.

- Boore D.M., Atkinson G.M. [2008] "Ground-motion prediction equations for the average horizontal component of PGA, PGV, and 5%-damped PSA at spectral periods between 0.01s and 10.0s," *Earthquake Spectra*, Vol. 24, pp. 99–138.
- Boore D.M., Joyner W.B., Fumal T.E. [1997] "Equations for estimating horizontal response spectra and peak acceleration from western North American earthquakes: A summary of recent work," *Seismological Research Letters*, Vol. 68, No. 1, pp. 128–153.
- Boore D.M., Watson-Lamprey J., Abrahamson N.A. [2006] "GMRotD and GMRotI: Orientation independent measures of ground motion," *Bulletin of the Seismological Society of America*, Vol. 96, pp. 1502–1511.
- Boore D.M., Azari A., Akkar S. [2012] "Using pad-stripped acausally filtered strong-motion data," *Bulletin of the Seismological Society of America*, Vol. 102, No. 2, pp. 751–760.
- Bozorgnia Y., Campbell K.W. [2004a] "Engineering characterization of ground motion," Chapter 5 in *Earthquake Engineering: From Engineering Seismology to Performance-Based Engineering* (Eds. Y. Bozorgnia and V.V. Bertero), CRC Press.
- Bozorgnia, Y. and Campbell KW [2004b]. "The vertical-to-horizontal spectral ratio and tentative procedures for developing simplified V/H and vertical design spectra," *Journal of Earthquake Engineering* Vol. 4, No. 4, pp. 539–561.
- Bozorgnia Y., Hachem M.H., Campbell K.W. [2010] "Ground motion prediction equation ("attenuation relationship") for inelastic response spectra," *Earthquake Spectra*, Vol. 26, No. 1, pp. 1–23.
- Bray J.D., Rodriguez-Marek A. [2004] "Characterization of forward-directivity ground-motions in the near-fault region," *Soil Dynamics and Earthquake Engineering*, Vol. 24, pp. 818–828.
- Brillinger D.R. Preisler H.K. [1984] "An exploratory analysis of the Joyner-Boore attenuation data," *Bulletin of the Seismological Society of America*, Vol. 74, pp. 1441–1450.
- Brillinger D.R., Preisler H.K. [1985] "Further analysis of the Joyner- Boore attenuation data," *Bulletin of the Seismological Society of America*, Vol. 75, No. 4, pp. 611–614.
- Brune J.N. [1970] "Tectonic stress and the spectra of seismic shear waves from earthquakes," *Journal of Geophysical Research*, Vol. 75, pp. 4997–5002.
- Brune J.N. [1971] "Correction," *Journal of Geophysical Research*, Vol. 76, pp. 5002.
- Budnitz R.J., Apostolakis G., Boore D.M., Cluff L.S., Coppersmit K.J., Cornell C.A., Morris P.A. [1997] "Recommendations for probabilistic seismic hazard analysis: Guidance on uncertainty and use of experts," *US Nuclear Regulatory Commission Report, NUREG/CR-6372*.
- Burkett E.R., Billen M.I. [2009] "Dynamics and implications of slab detachment due to ridge-trench collision," *Journal of geophysical Research*, Vol. 114, No. B12, doi: 10.1029/JB006402.
- Cameron W.I., Green R.U. [2007] "Damping correction factors for horizontal ground-motion response spectra," *Bulletin of the Seismological Society of America*, Vol. 97, No. 3, pp. 934–960.

- Campbell K.W. [1981] "A ground motion model for the central United States based on near-source acceleration data," *Proceeding of the Conference on Earthquakes and Earthquake Engineering: the Eastern United States*, Vol. 1, Ann Arbor Science Publishers, Ann Arbor, Michigan, pp. 213–232.
- Campbell K.W. [1981] "Near-source attenuation of peak horizontal acceleration," *Bulletin of the Seismological Society of America*, Vol. 71, pp. 2039–2070.
- Campbell K.W. [1982] "A preliminary methodology for the regional zonation of peak ground acceleration," *Proceedings of the 3rd International Earthquake Microzonation Conference*, University of Washington, Seattle, pp. 365–376.
- Campbell K.W. [1985] "Strong motion attenuation relations: A ten-year perspective," *Earthquake Spectra*, Vol. 1, No. 4, pp. 759–804.
- Campbell K.W. [1987] "Predicting strong ground motion in Utah," in *Assessment of Regional Earthquake Hazards and Risk along the Wasatch Front, Utah*, (Eds., P.L. Gori and W.W. Hays), *USGS Open-File Rept. 87–585*, Vol. 2, L1–L90.
- Campbell K.W. [1997] "Empirical near-source attenuation relationships for horizontal and vertical components of peak ground acceleration, peak ground velocity, and pseudo-absolute acceleration response spectra," *Seismological Research Letters*, Vol. 68, No. 1, pp. 154–179.
- Campbell K.W. [2000] "Predicting strong ground motion in Utah," in *Assessment of Regional Earthquake Hazards and Risk Along the Wasatch Front, Utah*, (Eds., P.L. Gori and W.W. Hays), *USGS Professional Paper 1500-L*, pp. L1–L31.
- Campbell K.W. [2001a] "Hybrid empirical model for estimating strong ground motion in regions of limited strong-motion recordings," *Proceedings of the OECD/NEA Workshop on the Engineering Characterization of Seismic Input*, Vol. 1, NEA/CSNI/R(2000)2, Nuclear Energy Agency, Paris, pp. 315–332.
- Campbell K.W. [2001b] "Development of semi-empirical attenuation relationships for the CEUS," *Final Report*, U.S. Geological Survey, Award 01HQGR0011.
- Campbell K.W. [2003a] "Prediction of strong ground motion using the hybrid empirical method and its use in the development of ground-motion (attenuation) relations in Eastern North America," *Bulletin of the Seismological Society of America*, Vol. 93, pp. 1012–1033.
- Campbell K.W. [2003b] "Erratum to Prediction of strong ground motion using the hybrid empirical method and its use in the development of ground-motion (attenuation) relations in Eastern North America," *Bulletin of the Seismological Society of America*, Vol. 93, pp. 1012–1033.
- Campbell KW [2011] "Ground motion simulation using hybrid empirical method: issues and insights," (Eds. S. Akkar, P. Gülkan and T. van Eck), Springer, GGEE 14, pp. 81–98.
- Campbell K.W., Duke C.M. [1974] "Bedrock intensity attenuation and site factors from San Fernando earthquake records," *Bulletin of the Seismological Society of America*, Vol. 64, pp. 173–185.

- Campbell K.W., Bozorgnia Y. [2007] "Campbell-Bozorgnia NGA ground motion relations for the geometric mean horizontal component of peak and spectra ground motion parameters," *PEER Report 2007/02*, Pacific Earthquake Engineering Research Center, Berkeley, CA, 240 pgs.
- Campbell K.W., Bozorgnia Y. [2008] "NGA ground motion model for the geometric mean horizontal component of PGA, PGV, PGD and 5% damped linear elastic response spectra for periods ranging from 0.01 to 10 s," *Earthquake Spectra*, Vol. 24, pp. 139–171.
- Campbell K.W., Bozorgnia Y. [2010] "A ground motion prediction equation for the horizontal component of cumulative absolute velocity (CAV) based on the PEER-NGA strong motion database," *Earthquake Spectra*, Vol. 26, pp. 635–650.
- Campbell K.W., Bozorgnia Y. [2011a]. "Empirical correlation of standardized cumulative absolute velocity (CAV) and seismic intensity based on the PEER-NGA database," *Earthquake Spectra*, Vol. 28, No. 2, pp. 457–485.
- Campbell K.W., Bozorgnia Y. [2011b] "Predictive equations for the standardized version of cumulative absolute velocity as adapted for use in the shutdown of U.S. nuclear power plants," *Nuclear Engineering and Design*, Vol. 241, pp. 2558–2569.
- Campbell K.W., Bozorgnia Y. [2012]. "A comparison of ground motion prediction equations for Arias intensity and cumulative absolute velocity developed using a consistent database and functional form," *Earthquake Spectra*, Vol. 28, No. 3, pp. 931–941.
- Cauzzi C., Faccioli E., Costa G [2011] "1D and 2D site amplification effects at Tarcento (Friuli, NE Italy), 30 years later," *Journal of Seismology*, Vol. 15, pp. 1–17.
- Chatelain J.L., Molnar P., Prévot R., Isacks B. [1992] "Detachment of part of the down-going slab and uplift of the New Hebrides (Vanuatu) Islands," *Geophysical Research Letters*, Vol. 19, pp. 1507–1510.
- Chen X. [1995] "Near-field ground motion from the Landers earthquake," *EERL 95-02*, Earthquake Engineering Research Laboratory, California Institute of Technology, Pasadena, CA.
- Chiou B., Youngs R.R., Abrahamson N.A., Addo K [2010]. "Ground-motion attenuation model for small-to-moderate shallow crustal earthquakes in California and its implications on regionalization of ground-motion prediction models," *Earthquake Spectra*, Vol. 26, pp. 907–926.
- Cloos M., Sapiie B., van Ufford A.Q., Weiland R.J., Warren P.Q., McMahon T.P. [2005] "Collisional delamination in New Guinea: The geotectonics of subducting slab breakoff," *Geological Society of America Special Paper* 400, 51 pgs.
- Cotton F., Pousse G., Bonilla F., Scherbaum F. [2008] "On the discrepancy of recent European ground-motion observations and predictions from empirical models: analysis of KIK-net accelerometric data and point-sources stochastic simulations," *Bulletin of the Seismological Society of America*, Vol. 98, No. 5, pp. 2244–2261.
- Delavaud E., Cotton F., Akkar S., Scherbaum F., Danciu L., Beauval C., Drouet S., Douglas J., Basili R., Sandikkaya M.A., Segou M., Faccioli E., Theodoulidis N. [2012] "Toward a ground-motion logic tree for probabilistic seismic hazard assessment in Europe," *Journal of Seismology*, Vol. 16, pp. 451–473.



- De Natale G., Faccioli E., Zollo A. [1988] "Scaling of peak ground motions from digital recordings of small earthquakes at Campi Flegrei, southern Italy," *Pure and Applied Geophysics*, Vol. 126, pp. 37–53.
- Dhakal J.P., Takai N., Sasatani T. [2010] "Empirical analysis of path effects on prediction equations of pseudo-velocity response spectra in northern Japan source," *Earthquake Engineering and Structural Dynamics*, Vol. 39, pp. 443–461.
- Douglas J. [2011] "Ground-motion prediction equations: 1964-2010," *Final report*, BRGM/RP-59356-FR.
- Douglas J., Smit P.M. [2001] "How accurate can strong ground motion attenuation relations be?" *Bulletin of the Seismological Society of America*, Vol. 91, pp. 1917–1923.
- Douglas J., Boore D.M. [2011] "High-frequency filtering of strong-motion records." *Bulletin of Earthquake Engineering*, Vol. 9, pp. 395–409.
- Douglas J., Jousset P. [2011] "Modeling the difference in ground-motion magnitude-scaling in small and large earthquakes," *Seismological Research Letters*, Vol. 82, pp. 504–508.
- Douglas J., Aochi H. [2008] "A survey of techniques for predicting earthquake ground motions for engineering purposes," *Surveys in Geophysics*, Vol. 29, pp. 187–220.
- Douglas J., Bungum H., Scherbaum F. [2006] "Ground-motion prediction equations for Southern Spain and Southern Norway obtained using the composite model perspective," *Journal of Earthquake Engineering*, Vol. 10, pp. 33–72.
- Douglas J., Faccioli E., Cotton F., Cauzzi C. [2009] "Selection of ground-motion prediction equations for GEM1," *GEM Technical Report*, GEM Foundation, Pavia, Italy.
- Douglas J., Cotton E.F., Di Alessandro C., Boore D.M., Abrahamson N.A. [2011] "Pre-selection of ground-motion prediction equations for Task 2 of the GEM Global GMPEs project," *Technical Report to PEER*, Berkeley, CA.
- Electric Power Research Institute [2004]. "CEUS ground motion project final report," *Tech. Rept. 1009684*, EPRI, Palo Alto, CA, Dominion Energy, Glen Allen, VA, Entergy Nuclear, Jackson, MS, and Exelon Generation Company, Kennett Square, PA.
- Facenna C., Bellier O., Martinod I., Piromallo C., Reagard V. [2005] "Slab detachment beneath eastern Anatolia: A possible cause for the formation of the North Anatolian fault," *Earth and Planetary Science Letters*, Vol. 242, pp. 85–97.
- Frankel A. [2009]. "A constant stress-drop model for producing broadband synthetic seismograms: Comparison with the Next Generation Attenuation relations," *Bulletin of the Seismological Society of America*, Vol. 99, pp. 664–680.
- Frohlich C., Apperson K.D. [1992] "Earthquake focal mechanisms, moment tensors, and the consistency of seismic activity near plate boundaries," *Tectonics*, Vol. 11, pp. 279–296.
- Frohlich C., Kadinsky-Cade K., Davis S.D. [1995] "A re-examination of the Bucaramanga, Colombia, earthquake nest," *Bulletin of the Seismological Society of America*, Vol. 85, pp. 1622–1634.



- Graves R.W., Pitarka A. [2004]. "Broadband time history simulation using a hybrid approach," *Proceedings of the 13th World Conference on Earthquake Engineering*, Paper No. 1098, Vancouver, B.C.
- Graves R.W., Pitarka Aa [2010]. "Broadband ground-motion simulation using a hybrid approach," *Bulletin of the Seismological Society of America*, Vol. 100, pp. 2095–2123.
- Gülerce Z., Abrahamson N.A. [2011] "Site-specific spectra for vertical ground motion," *Earthquake Spectra*, Vol. 27, pp. 1023–1047.
- Hanks T.C. [1979] "b values and  $\omega$ - $\gamma$  seismic source models: Implications for tectonic stress variations along active crustal fault zones and the estimation of high-frequency strong ground motion," *Journal of Geophysical Research*, Vol. 84, pp. 2235–2242.
- Hanks T.C., McGuire R.K. [1981] "The character of high-frequency strong ground motion," *Bulletin of Seismological Society of America*, Vol. 71, pp. 2071–2095.
- Hartzell S.H. [1978] "Earthquake aftershocks as Green's functions," *Geophysical Research Letters*, Vol. 5, pp. 1–14.
- Hartzell S.H., Heaton T. [1995] "San Andreas deterministic fault problem Green's function summation for a finite source," *Proceedings of the Modelling Earthquake Ground Motion at Close Distance*, (Eds. J.F. Schneide and P.G. Somerville), *Abstract No. TR-104975*, Electric Power Research Institute, Palo Alto, CA.
- Hartzell S.H., Harmsen S., Frankel A., Larsen S. [1999] "Calculation of broadband time histories of ground motion: comparison of methods and validation using strong-ground motion from the 1994 Northridge earthquake," *Bulletin of the Seismological Society of America*, Vol. 89, pp. 1484–1504.
- Iwan W.D. Moser M.A., Peng C.-Y. [1985] "Some observations on strong-motion earthquake measurement using a digital accelerograph," *Bulletin of the Seismological Society of America*; Vol. 75, pp. 1225–1246.
- Irikura K. [1986] "Prediction of strong acceleration motions using empirical Green's function," *Proceedings of the 7th Japan Earthquake Engineering Symposium*, pp. 151–156.
- Irikura K. Miyake H. [2001] "Prediction of strong ground motion for scenario earthquakes," *Journal of Geographical Sciences*, Vol. 110, pp. 849–875 (in Japanese).
- Irikura K. Miyake H. [2011] "Recipe for predicting strong ground motion from crustal earthquake scenarios," *Pure Applied Geophysics*, Vol. 168, pp. 85–104.
- Jayaram N., Baker J.W. [2010] "Considering spatial correlation in mixed-effects regression and the impact on ground-motion models," *Bulletin of the Seismological Society of America*; Vol. 100, No. 6, pp. 3295–3303.
- Johnston A.C., Coppersmith K.J., Kanter L.R. Cornell C.A. [1994] "The earthquakes of stable continental regions: Assessment of large earthquake potential," *TR-102261*, Vol. 1–5 (Ed. J.F. Schneider), Electric Power Research Institute, Palo Alto, CA.
- Joyner W.B., Boore D.M. [1981] "Peak horizontal acceleration and velocity from strong-motion records including records from the 1979 Imperial Valley, California, earthquake," *Bulletin of the Seismological Society of America*, Vol. 71, No. 6, pp. 2011–2038.

- Joyner W.B., Boore D.M. [1993] "Methods for regression analysis of strong-motion data," *Bulletin of the Seismological Society of America*, Vol. 83, No. 2, pp. 469–487.
- Kaklamanos J., Baise L.G., Boore D.M. [2011] "A framework for estimating unknown input parameters when implementing the NGA ground motion prediction equations in engineering practice," *Earthquake Spectra*, Vol. 27, No. 4, pp. 1219–1235.
- Kamae K., Irikura K., Pitarka A. [1998]. "A technique for simulating strong ground motions using hybrid Green's functions," *Bulletin of the Seismological Society of America*, Vol. 88, pp. 357–367.
- Kayen R.E., Mitchell J.K. [1997] "Assessment of liquefaction potential during earthquakes by Arias Intensity," *Journal of Geotechnical and Geoenvironmental Engineering (ASCE)*, Vol. 123, pp. 1162–1174.
- Lee V.W., Trifunac M.D. [1990] "Automatic digitization and processing of accelerograms using PC," *Report No. 90-03*, Department of Civil Engineering, University of Southern California, Los Angeles, CA.
- Leonard M. [2010] Earthquake fault scaling: Self-consistent relating of rupture length, width, average displacement, and moment release," *Bulletin of the Seismological Society of America*, Vol.100, pp. 1971-1988.
- Levin V., Shapiro N., Park J. Ritzwoller M. [2002] "Seismic evidence for catastrophic slab loss beneath Kamchatka," *Nature*, Vol. 418, pp. 763–767.
- Lin Y.Y., Miranda E., Chang K.C. [2005] "Evaluation of damping reduction factors for estimating elastic response of structures with high damping," *Earthquake Engineering and Structural Dynamics*, Vol. 34, No. 11, pp. 1427–1443.
- Liu A.H., Stewart J.P., Abrahamson N.A., Moriwaki Y. [2001] "Equivalent number of uniform stress cycles for soil liquefaction analysis," *Journal of Geotechnical and Geoenvironmental Engineering*, Vol. 127, No. 12, pp. 1017–1026.
- Luzi L., Hailemichael S., Bindi D., Pacor F., Mele F., Sabetta F. [2008] "ITACA (Italian Accelerometric Archive): a web portal for the dissemination of Italian strong-motion data," *Seismological Research Letters*, Vol. 79, No. 5, pp. 716–722.
- Marra F., Azzara R., Bellucci F., Caserta A., Cultrera G., Mele, B., Palombo B., Rovelli A., Boschi E. [2000] "Large amplification of ground motion at rock sites within a fault zone in Nocera Umbra (central Italy)," *Journal of Seismology*, Vol. 4, pp. 543–554.
- McGuire R.K. Hanks T.C. [1980] "RMS accelerations and spectral amplitudes of strong ground motion during the San Fernando, California, earthquake," *Bulletin of Seismological Society of America*, Vol. 70, pp. 1907–1919.
- McVerry G.H., Zhao J.X., Abrahamson N.A., Somerville P.G. [2006] "New Zealand acceleration response spectrum attenuation relations for crustal and subduction zone earthquakes", *Bulletin of the New Zealand Society for Earthquake Engineering*, Vol. 39, No.4, pp. 1–58.
- Midorikawa S., Ohtake Y. [2004] "Variance of peak ground acceleration and velocity in attenuation relationships," *Proceedings of the 13th World Conference on Earthquake Engineering*, Paper No. 325, Vancouver, B.C.

- Motazedian D. [2002] "Development of earthquake ground motion relations for Puerto Rico," Ph.D. Thesis, Carleton University, Ottawa, Ontario, Canada.
- Motazedian D., Atkinson G.M. [2005] "Stochastic finite-fault model based on dynamic corner frequency," *Bulletin of Seismological Society of America*, Vol. 95, pp. 995–1010.
- Munson C, Thurber C. [1997] "Analysis of the attenuation of strong ground motion on the Island of Hawaii," *Bulletin of the Seismological Society of America*, Vol. 87, No. 4, pp. 945–960.
- Ordaz M., Reyes C. [1999] "Earthquake hazard in Mexico City: Observations versus computations," *Bulletin of the Seismological Society of America*, Vol. 89, No. 5, pp. 1379–1383.
- Paciello A., Rinaldis D., Romeo R. [2000] "Incorporating ground motion parameters related to earthquake damage into seismic hazard analysis," *Proceedings of the Sixth International Conference on Seismic Zonation: Managing Earthquake Risk in the 21st Century*, Earthquake Engineering Research Institute, Oakland, CA.
- Pacor F., Cultrera G., Mendez A., Cocco M. [2005] "Finite fault modeling of strong ground motions using a hybrid deterministic–stochastic approach," *Bulletin of the Seismological Society of America*, Vol. 95, pp. 225–240.
- Paolucci R., Rovelli A., Faccioli E., Cauzzi C., Finazzi D., Vanini M., Di Alessandro C., Calderoni G. [2008] "On the reliability of long period spectral ordinates from digital accelerograms," *Earthquake Engineering and Structural Dynamics*, Vol. 37, pp. 697–710.
- Petersen M., Frankel A., Harmsen S., Mueller C., Haller K., Wheeler R., Wesson R., Zeng Y., Boyd O., Perkins D., Luco N., Field E., Wills C., Rukstales K. [2008] "Documentation for the 2008 Update of the United States National Seismic Hazard Maps," *U.S. Geological Survey, Open-File Report 08-1128*.
- Pezeshk S., Zandieh A., Tavakoli B. [2011]. "Hybrid empirical ground-motion prediction equations for Eastern North America using NGA models and updated seismological parameters," *Bulletin of the Seismological Society of America*, Vol. 101, pp. 1859–1870.
- Pousse G., Bonilla F.L., Cotton F., Margerin L. [2006] "Nonstationary stochastic simulation of strong ground motion time histories including natural aariability: Application to the K-Net Japanese database," *Bulletin of the Seismological Society of America*, Vol. 96, No. 6, pp. 2103–2117.
- Power M., Chiou B., Abrahamson N.A., Bozorgnia Y., Shantz T., Roblee C. [2008] "An overview of the NGA project," *Earthquake Spectra*, Vol. 24, No. 1, pp. 3–21.
- Radiguet M., Cotton F., Manighetti I., Campillo M., Douglas J. [2009] "Dependency of near-field ground motions on the structural maturity of the ruptured faults," *Bulletin of the Seismological Society of America*, Vol. 99, pp. 2572–2581.
- Richter C.F. [1935] "An instrumental magnitude scale," *Bulletin of the Seismological Society of America*, Vol. 25, pp. 1–32.
- Rhoades D.A. [1997] "Estimation of attenuation relations for strong motion data allowing for individual earthquake magnitude uncertainties," *Bulletin of the Seismological Society of America* Vol. 87, No. 6, pp. 1674–1678.

- Rodriguez-Marek A., Montalva G.A., Cotton F., Bonilla F. [2011] "Analysis of single-station standard deviation using the Kik-net data, *Bulletin of the Seismological Society of America* Vol. 101, pp. 1242–1258, doi: 10.1785/0120100252.
- Rowshandel B. [2006]. "Incorporating source rupture characteristics into ground motion hazard analysis models," *Seismological Research Letters*, Vol. 77, pp. 708–722.
- Rowshandel B. [2010]. "Directivity correction for the Next Generation Attenuation (NGA) relations", *Earthquake Spectra*, Vol. 26, No. 2, pp. 525–559.
- Ruiz-Garcia J., Miranda E [2007] "Probabilistic estimation of maximum inelastic displacement demands for performance-based design," *Earthquake Engineering Structural Dynamics*, Vol. 36, No. 9, pp. 1235–1254.
- Sadigh K., Chang C.-Y., Egan J.A., Makdisi F., Youngs R.R. [1997] "Attenuation relationships for shallow crustal earthquakes based on California strong motion data," *Seismological Research Letters*, Vol. 68, No. 1, pp. 180–189.
- Sandikkaya A.M., Akkar S., Bard P.-Y. [2012] "A nonlinear site amplification model for the new pan-European ground-motion prediction equations," *Bulletin of the Seismological Society of America*, Vol. 103, No. 1, pp. 19–32.
- Savy J., Foxall W., Abrahamson N.A. [1999] "Guidance for performing probabilistic seismic hazard analysis for a nuclear plant site: Example application to the southeastern United States," *NUREG/CR-6607*, U.S. Nuclear Regulatory Commission, Washington, D.C.
- Scherbaum F., Schmedes J., Cotton F. [2004] "On the conversion of source-to-site distance measures for extended earthquake source models," *Bulletin of the Seismological Society of America*, Vol. 94, pp. 1053–1069.
- Scherbaum F., Bommer J.J., Bungum H., Cotton F., Abrahamson N.A. [2005] "Composite ground-motion models and logic trees: methodology, sensitivities, and uncertainties," *Bulletin of the Seismological Society of America*, Vol. 95, No. 5, pp. 1575–1593.
- Scherbaum F., Cotton F. Staedtke H. [2006] "The estimation of minimum-misfit stochastic models from empirical ground-motion prediction equations," *Bulletin of Seismological Society of America*, Vol. 96, pp. 427–445.
- Seed H.B., Idriss I.M. [1971] "Simplified procedure for evaluating soil liquefaction potential," *Journal of the Soil Mechanics and Foundations Division, ASCE*, Vol. 97 (SM9), pp. 1249–1273.
- Silva W.J., Gregor N., Darragh R. [2002] "Development of regional hard rock attenuation relations for central and eastern North America," report prepared by Pacific Engineering and Analysis, El Cerrito, CA.
- Silva W.J., Abrahamson N.A., Toro G., Costantino C. [1996] "Description and validation of the stochastic ground motion model," *Report to Brookhaven National Laboratory, Associated Universities, Inc., Upton, NY*.
- Skarlatoudis A.A., Papazachos C.B., Margaris B.N. [2003] "Determination of noise spectra from strong motion data recorded in Greece," *Journal of Seismology*, Vol. 7, pp. 533–540.

- Sokolov V., Bonjer K.P., Wenzel F., Grecu B., Mircea R. [2008]. "Ground-motion prediction equations for the intermediate depth Vrancea (Romania) earthquakes," *Bulletin of Earthquake Engineering*, Vol. 6, No.3, pp. 367–388.
- Somerville P.G. [2003] "Magnitude scaling of the near fault rupture directivity pulse," *Physics of the Earth and Planetary Interiors*, Vol. 137, No. 1, pp. 201–212.
- Somerville P.G., Smith N.F., Graves R.W., Abrahamson N.A. [1997] "Modification of empirical strong ground motion attenuation relations to include the amplitude and duration effects of rupture directivity," *Seismological Research Letters*, Vol. 68, No. 1, pp. 199–222.
- Somerville P.G., Irikura K., Graves R.W., Sawada S., Wald D., Abrahamson N.A., Iwasaki Y., Kagawa T., Smith N.F., Kowada A. [1999] "Characterizing earthquake slip models for the prediction of strong ground motion," *Seismological Research Letters*, Vol. 70, pp. 59–80.
- Somerville P.G., Collins N., Abrahamson N.A., Graves R.W., Saikia C. [2001] "Ground motion attenuation relations for the Central and Eastern United States," *Final Report to the U.S. Geological Survey*, Contract No. 99HQGR0098.
- Somerville P.G., Graves R.W., Collins N., Song S.G., Ni S., Cummins P. [2009] "Source and ground motion models of Australian earthquakes", *Proceedings of the 2009 Annual Conference of the Australian Earthquake Engineering Society*, Newcastle, Australia.
- Spudich P., Chou B.S.J. [2008] "Directivity in NGA earthquake ground motions: Analysis using Isochrone Theory," *Earthquake Spectra*, Vol. 24, No. 1, pp. 279–298.
- Stewart J., Boore D.M., Campbell K., Erdik M., Silva W.J. [2011] "Estimating site effects in parametric ground-motion models," for Task 1.b of the GEM Global GMPEs project," *Technical Report to PEER*, Berkeley, CA.
- Sunder S.S., Connor J.J. [1982] "A new procedure for processing strong-motion earthquake signals," *Bulletin of the Seismological Society of America*, Vol. 72, pp. 643–661.
- Stafford P.J., Mendis R., Bommer J.J. [2008] "Dependence of damping correction factors to response spectra on duration and number of cycles," *Journal of Structural Engineering, ASCE*, Vol. 134, No. 8, pp. 1364–1373.
- Stafford P.J., Bommer J.J. [2009] "Empirical equations for the prediction of the equivalent number of cycles of earthquake ground motion," *Soil Dynamics and Earthquake Engineering*, Vol. 29, No. 11-12, pp. 1425–1436.
- Stepp J., Wong I., Whitney J., Quittmeyer R., Abrahamson N.A., Toro G., Youngs R., Coppersmith K., Savy J., Sullivan T., and Yucca Mountain PSHA Project Members [2001] "Probabilistic seismic hazard analyses for ground motions and fault displacement at Yucca Mountain, Nevada," *Earthquake Spectra*, Vol. 17, pp. 113–151.
- Strasser F., Abrahamson N.A., Bommer J.J. [2009] "Sigma: issues, insights, and challenges," *Seismological Research Letters*, Vol. 80, No. 1, pp. 40–56.
- Tavakoli S., Pezeshk S. [2005] "Empirical-stochastic ground-motion prediction for eastern North America," *Bulletin of the Seismological Society of America*, Vol. 95, pp. 2283–2296

- Tothong P., Cornell C.A. [2006] "An empirical ground motion attenuation relation for inelastic spectral displacement," *Bulletin of the Seismological Society of America*, Vol. 96, No. 6, pp. 2146–2164.
- Travasarou T., Bray J.D., Abrahamson N.A. [2003] "Empirical attenuation relationship for Arias intensity," **Error! Reference source not found.**, Vol. 32, pp. 1133–1155.
- Trifunac M.D. [1971] "Zero baseline correction of strong-motion accelerograms," *Bulletin of the Seismological Society of America*, Vol. 61, pp. 1201–1211.
- Trifunac M.D. [1973] "Routine computer processing of strong-motion accelerograms," *EERL 73-03*, Earthquake Engineering Research Laboratory, California Institute of Technology, Pasadena, CA.
- Trifunac M.D., Lee V.W., Todorovska M.I. [1999] "Common problems in automatic digitization of strong motion accelerograms," *Soil Dynamics and Earthquake Engineering*, Vol. 18, pp. 519–530.
- Trifunac M.D., Todorovska M.I. [2001] "A note on the usable dynamic range of accelerographs recording translation," *Soil Dynamics and Earthquake Engineering*, Vol. 21, pp. 275–286.
- Van Houtte C., Drouet S., Cotton F. [2011] "Analysis of the origins of  $\kappa$  (Kappa) to compute hard rock to rock adjustment factors for GMPEs," *Bulletin of the Seismological Society of America*, Vol. 101, No. 6, pp. 2926–2941.
- Yenier E., Sandikkaya M.A., Akkar S. [2010] "Report on the fundamental features of the extended strong motion databank prepared for the SHARE project," SHARE Report, 44 pgs.
- Youngs R.R., Abrahamson N.A., Makdisi F.I., Singh K. [1995] "Magnitude-dependent variance of peak ground acceleration," *Bulletin of the Seismological Society of America*, Vol. 85, pp. 1161–1176.
- Wald D.J., Quitoriano V., Heaton T.H., Kanamori H. [1999] "Relationships between peak ground acceleration, peak ground velocity, and Modified Mercalli Intensity in California," *Earthquake Spectra*, Vol. 15, pp. 557–564.
- Watson-Lamprey J., Boore, D.M. [2007] "Beyond SaGMRotI: Conversion to SaArb, SaSN, and SaMaxRot," *Bulletin of the Seismological Society of America*, Vol. 97, pp. 1511–1524.
- Wilson R.C. Keefer D.K. [1985] "Predicting areal limits of earthquake-induced land sliding," in "Evaluating Earthquake Hazards in the Los Angeles Region-An Earth-Science Perspective," (Ed. J.I. Ziony) *USGS Professional Paper 1360*.
- Wong I.G., Chapman D.S. [1990] "Deep intraplate earthquakes in the western United States and their relationship to lithospheric temperatures," *Bulletin of the Seismological Society of America*, Vol. 80, pp. 589–599.
- Wortel M.J.R., Spakman W. [2000] "Subduction and slab detachment in the Med.-Carp. region," *Science*, Vol. 290, pp. 1910–1917.
- Wu Y.-M., Wu C.-F. [2007] "Approximate recovery of co-seismic deformation from Taiwan strong-motion records," *Journal of Seismology*, Vol. 11, pp. 159–170.
- Utsu T. [2002] "Relationships between magnitude scales," in *International Handbook of Earthquake and Engineering Seismology-Part A* (Eds. W.H.K. Lee WHK, H. Kanamori, P.C. Jennings, and C. Kisslinger), pp. 733–746.

- Zeng Y., Chen C.-H. [2001] "Fault rupture process of the 20 September 1999 Chi-Chi, Taiwan, earthquake," *Bulletin of the Seismological Society of America*, Vol. 91, pp. 1088–1098.
- Zhao J.X. [2010] "Geometric spreading functions and modeling of volcanic zones for strong-motion attenuation models derived from records in Japan," *Bulletin of the Seismological Society of America*, Vol. 100, No. 2, pp. 712–732.
- Zhao J.X., Zhang J., Asano A., Ohno Y., Oouchi T., Takahashi T., Ogawa H., Irikura K., Thio H.K., Somerville P.G., Fukushima Y. [2006] "Attenuation relations of strong ground motion in Japan using site classification based on predominant period," *Bulletin of the Seismological Society of America*, Vol. 96, pp. 898–913.
- Zoback ML [1992] "First- and second-order patterns of stress in the lithosphere: The World Stress Map Project," *J. Geophysical Research*, Vol. 97, No. 11, pp. 703–728.

### Website references

#### 1. SHARE

*Seismic Harmonization in Europe*

[Available at <http://www.share-eu.org>]

#### 2. OPENQUAKE

*Open-source software Openquake to compute seismic hazard and risk*

[Available at <http://openquake.org>]

#### 3. ITACA

*Italian accelerometric archive*

[Available at <http://itaca.mi.ingv.it/ItacaNet/>]

#### 4. NGA West Project

*Next Generation Attenuation (NGA) West project*

[Available at <http://peer.berkeley.edu/ngawest/>]

#### 5. David Boore Online Software – NGA\_GM\_TMR

*Implementation of NGA models for specified Period, Magnitude and Distance*

[Available at [http://daveboore.com/software\\_online.htm/](http://daveboore.com/software_online.htm/)]